THE DISINTEGRATION OF NEON BY FAST NEUTRONS

by

LOUIS FERDINAND MONIER
B.A.Sc., University of Montreal, 1957

A thesis submitted in partial fulfilment of the requirements for the degree of

MASTER IN APPLIED SCIENCE

in

PHYSICS

We accept this thesis as conforming to the required standard

THE UNIVERSITY OF BRITISH COLUMBIA

April, 1960

In presenting this thesis in partial fulfilment of the requirements for an advanced degree at the University of British Columbia, I agree that the Library shall make it freely available for reference and study. I further agree that permission for extensive copying of this thesis for scholarly purposes may be granted by the Head of my Department or by his representatives. It is understood that copying or publication of this thesis for financial gain shall not be allowed without my written permission.

Department of **Physics**

The University of British Columbia,
Vancouver 8, Canada.

Date **April 25th, 1960**

ABSTRACT

A study has been made of the fast neutron induced reactions in natural neon gas. The neon was contained in a cylindrical geometry fast gridded ionization chamber, and the irradiating monokinetic neutrons were obtained by bombarding thin heavy ice targets with monokinetic deuterons accelerated by the U.B.C. Van de Graaff accelerator. Pulse height analysis, after amplification of the pulses, gave the energy distribution of the induced reactions, the primary reaction proceeding being $Ne^{20}(n,\alpha)O^{17}$, with two alpha groups resulting from transitions to both the ground and first excited state of the O^{17} nucleus. The excitation function showed the existence of resonances in the Ne^{21} compound nucleus at the following energies, in Mev 10.04, 10.20, 10.32, 10.46, 10.63, 10.90, 11.06, 11.33, 11.44, 11.63, 11.76, 11.88, 11.96, 12.05 and 12.24. The total (n,α) cross section varies from 90 mb to 500 mb in this energy range.

TABLE OF CONTENTS

LIST OF ILLUSTRATIONS

Figures ff. p. 52

Plates Map Cabinet 8

ACKNOWLEDGEMENTS

The author is pleased to express his gratitude to Dr. J. B. Warren, for his kind supervision of the work done in this thesis.

Thanks are due to Dr. B. L. White for many helpful discussions and suggestions.

Thanks are also due to Mr. P. S. Takhar for help in operating the Van de Graaff generator.

The author gratefully acknowledges the receipt of two scholarships from the National Research Council of Canada.

INTRODUCTION

Natural neon consists of those isotopes Ne^{20}, Ne^{21} and Ne^{22}. From neon and reaction data, it is possible to compute the approximate Q-values for all likely reactions which would occur with fast neutron irradiation with neutron energies from 3 Mev to 5.5 Mev, with the result shown in the table below:

Isotope	Abundance (%)	Reaction	Q-value (Mev)
Ne^{20}	90.92	(n, α)	-0.608
		(n,p)	-6.267
Ne^{21}	0.257	(n, α)	+0.704
		(n,p)	-4.945
Ne^{22}	8.82	(n, α)	-5.704
		(n,p)	-6

Thus with neutrons below 5.5 Mev energy, one would expect to find only $Ne^{20}(n, \alpha)$ disintegrations (excluding elastic and inelastic scattering).

The early work of Sikkema (1950) did in fact establish the occurrence of the $Ne^{20}(n, \alpha)$ reaction over the neutron energy range 2.2 to 3.4 Mev, and Barschall (1951) showed the existence of large resonances at 2.87 and 3.26 neutron bombarding energy. An estimate of the absolute cross section was also made by these others. Flack et al (1952), Warren and Erdman (1953) at this laboratory studied this reaction using a parallel plate geometry, fast gridded

ionization chamber and established the fact that the reaction proceeded to both the ground state and first excited state of O^{17} as well as the existence of numerous resonances over the neutron energy range 3 to 5 Mev. However, at that time, the stopping power of heavy ice was undergoing a rather major correction through the precise work of Whaling (1958) so that the absolute cross section data obtained by these workers did not appear to tally with the earliest work. Moreover, the parallel plate chamber displayed objectionable characteristics, the magnitude of the yield varying quite considerably depending on the orientation with respect to the neutron beam.

Recently Hay and Warren (1959) studied the photodisintegration of neon using a cylindrical geometry gridded ionisation chamber, which makes far better use of the available neon gas, and because of the size and higher pressure used had a relatively small wall effect. Because of the excellent resolution and performance of this chamber, it was decided to repeat the earlier measurements on the $Ne^{20}(n,\alpha)$ reaction under conditions of much higher energy resolution and stability than were possible in 1952. While this was underway some further preliminary data concerning the excitation function was published from the Rice Institute (Bonner et al, 1959), which confirmed many of the resonances previously found by the U.B.C. electrostatic generator group.

With the improvement in technique achieved, it was expected that the disintegration energies would be adequately

accurately known so as to provide a check on the mass values currently quoted for the isotopes involved, and also to establish the existence of relatively weak resonances together with the resonant energies with some moderate precision. Moreover, the increased detection sensitivity with the cylindrical chamber would enable very thin heavy ice targets to be used, and in this way to enable very closely monokinetic neutron beams to be employed for running over some of the major resonances to establish that the width observed was characteristic of the resonance and not due to finite neutron energy resolution. All this has in fact been accomplished together with an absolute cross section measurement. While in the absence of angular distribution data it is not possible to establish the angular momentum or parity characteristics of the levels found, the excitation function does give information concerning the level density and average level width in the region of excitation energy examined, and also the trend of the cross section with varying neutron energy which is of the type which has led to the "cloudy crystal ball" concept of a nucleus.

Chapter I

THE DISINTEGRATION DETECTOR

1. Choice of Detector

Since pure neon is an excellent counter gas except for its low breakdown potential, the disintegrations produced in neon by fast neutrons may be conveniently detected by means of an ionization chamber or proportional counter.

In order to keep the solid angle subtended at the target by the detecting chamber to a reasonably small value and to raise the sensitivity while at the same time reducing the wall effect, it is necessary to use neon at several atmosphere pressure. Under these circumstances, a simple ionization chamber becomes too "slow" a device since the pulse duration is set by the travel time of the positive ions. A proportional counter can be used but is rather sensitive to gas purity and the collector field near the outer wall is relatively low with field at the central wire adequate to give gas amplification factors of 10 to 100. A gridded ionization chamber thus seems the best choice for this type of study as it possesses the virtues of speed and better stability to impurities since no gas gain is involved. It suffers from the disadvantage of requiring a more complex high gain amplifier with low noise head amplifier, and much depends on the latter as the noise level settles the resolution obtainable.

Cylindrical geometry provides better use of the available neon gas as the dead space is less. Also even with disintegrations producing relatively long tracks, since so few end in the gridded shielded region, there can be little dependence of pulse rate on orientation with respect to the neutron beam.

2. Operation of the Gridded Ionization Chamber

A simple ionization chamber consists usually of two electrodes (collector or anode and cathode), having an inherent self capacity C. On the passage of a charged particle, positive ions and electrons are produced. In the presence of an electric field, the ions drift along the lines of force which start on the collector and end on the cathode. The drift velocity is proportional to the intensity of the electrostatic field and inversely proportional to the gas pressure. In rare gases, the negative ions are electrons which have a drift velocity of about 1000 times those of positive ions. The H.T. (high voltage supply) is connected to the collector through a large resistance R, so that the time constant CR is many times greater than the collection time T, The charge Ne collected produces a small voltage step on the collector of amplitude $\frac{Ne}{C}$. This voltage step then decays to zero with a time constant CR as the charge leaks away through the resistor R. To improve the resolving time of the chamber and amplifier combination, a shaping circuit (usually a differentiating circuit) is incorporated

which makes the trailing edge of the pulses fall as rapidly as possible.

If the pulse on the collector is differentiated by a time constant shorter than the collecting time of the positive ions, the amplitude of the pulses is no longer proportional to the total number of ion pairs produced, but is also a function of the distance from the collector at which the ionization occurs. As suggested by Frish, such a disadvantage may be removed by the introduction of a wire mesh shield grid close to the collector.

The grid is held at an intermediate potential between the positive collector and the earthed cathode which is in this case the casing of the chamber. When an ionizing event is produced, the electrons drift toward the grid and the positive ions in the opposite direction. During this process, no change is produced on the collector, since this is electrostatically screened by the grid from the induced effect of the electrons and the positive ions. Electrons in their drift pass through the grid, with only a very small percentage being captured by the grid. In this last region, the electrons begin to induce on the collector a charge which rises from zero to the full value Ne as the electrons move through the distance from the grid to the collector plate. In the same time, the voltage pulse rises to the amplitude $\frac{Ne}{C}$ and is uninfluenced by the positive ions left in the region between the casing and the grid.

The gridded chamber enables high resolving time and preserves relationship between pulse amplitude and particle energy.

3. Description

Figure 1 is a drawing of the chamber used. It was made from steel tubing with welded flanges. The wall thickness was reduced to 1/8" around the sensitive volume. The end plates were sealed with lead gasket, avoiding unnecessary exposure of the filling gas to rubber. A neoprene O-ring was placed outside the lead gasket, thus a vacuum of 10^{-6} mm of Hg was obtained. All interior surfases were coated with "aquadag" colloidal graphite, to reduce background from natural activity in the steel.

On one side of the chamber the gas purifier was permanently attached to the chamber: being in a vertical position, the convection currents assured circulation of gas from the chamber through the purifier. It was made of steel surrounded by a heating coil capable of raising the interior temperature of the purifier up to 350°C. Copper cooling coils placed at both ends were necessary to protect the O-ring seals in the ends of the purifier. The purifier contains a compound of calcium and magnesium known to be effective in removing impurities such as oxygen, nitrogen and water vapor from the counter gas.

A plutonium source, whose α-particles could be cut off by a magnetically operated shutter, was placed inside the

chamber, and used to provide an energy calibration for the ionization pulses.

The chamber had a sensitive volume of 4.06 liters and was filled with neon at 120 p.s.i.a. or 8.1 atmosphere pressure.

The design of the grid follows the recommendations of Bunemann, Cranshaw and Harvey (1949). The electrode system is shown in fig. 2. The collector was of Tungsten and the grid consisted of 36 strands of No. 36 wire (made by Johnson Matthey Co. Ltd.): grid collector spacing was 8.75 mm, and grid plate 6.75 cm. The grid potential was set at one half of the collector potential. Calculation shows that the grid shielding efficiency under these conditions was 0.94, and the transparency to electron was unity. See Appendix A.

4. Filling Gas

Neon is well suited for use in an ionization chamber, since electron attachment does not occur.

Although the purest obtainable gas was used, the purifier on the chamber was still necessary, because of occluded gases on the chamber walls, which enter the chamber gas after long periods, despite baking under a heat lamp prior to filling.

The maximum limits of possible impurity of the neon stated by the manufacturer (Matheson Co., for "Research

Grade") are:

Oxygen	0.0005	Mole percent
Hydrogen	0.0005	" "
Nitrogen	0.01	" "
Helium	0.03	" "

The chamber, after being evacuated and heated at a pressure as low as 10^{-6} mm of Hg for 5 days, was then filled by passing the gas through a liquid nitrogen cold trap to remove water vapour and any other condensed substances which might be present.

In order to increase the number of disintegrations per unit of time and to increase the number of events which are completely confined to the sensitive volume, the pressure had to be as high as possible. Neon being a costly rare gas the amount of neon available for this work was limited, and also by the pressure that the pot was able to hold. Unfortunately, due to some imperfection in the solder joint between the centre electrode and the top plate, 8.1 atmospheres was the maximum pressure which seemed advisable. Nevertheless, this pressure is quite satisfactory.

Since a normal mixture of neon contains three stable isotopes, a simple calculation gives the number of atoms of each neon isotope in the sensitive volume of the chamber.

Isotope	Abundance	No. of Atoms
Ne^{20}	90.92%	7.511×10^{23}
Ne^{21}	0.26%	0.021×10^{23}
Ne^{22}	8.82%	0.728×10^{23}

Chapter II

NEUTRON PRODUCTION

1. Production of Monoenergetic Fast Neutrons

For studying the interaction between neutrons and nuclei as a function of energy, a source of monoenergetic neutrons of variable energy is required. Such a source with large yield of neutrons and a reasonable energy range is obtainable from $D(d,n)He^3$ reaction. The energy of the incident particles was produced by accelerating deuterium ions by means of the Van de Graaff generator of U.B.C., which has a capacity of 2.3 Mev; this permits a range of neutron energy from 3.2 Mev to 5.5 Mev.

A solid heavy ice target was used instead of a gas target because an adequate neutron intensity would have required a relatively high gas pressure, which implies difficult construction.

However, in order to study a high energy spectrum, (about 16.7-Mev neutron energy), the reaction $d(T,n)He^4$ was also used.

2. $D(d,n)He^3$ Reaction

The neutron emitted are monoenergetic, but their energy is function of the energy of the incoming particle, and depends strongly on the angle of emission measured relatively to the deuteron beam. The extent to which the neutron energies are truly homogeneous thus depends on the energy

spread of the incoming deuterons, the thickness of the ice target and the smallness of the solid angle subtended by the chamber.

The determination of the energy of the neutrons, emitted from a given nuclear reaction as a function of the energy of the incident particle and the angle of emission, can be calculated from the equations for conservation of energy and momentum to be

$$En = \frac{Ed}{4}(\cos^2\theta + 1) + \frac{3}{4}Q \pm \frac{\sqrt{2Ed}}{2}\sqrt{\frac{Ed}{8}(\cos^2\theta + 2) + \frac{3}{4}Q}\cos\theta$$

where: En = neutron energy in the lab system

Ed = deuteron energy in the lab system

Q = Q-value of the $D(d,n)He^3$ reaction

Such a calculation including relativistic correction has been carried out by Fowler and Brolley (1956), using 3.2664 Mev for the Q-value. The results are tabulated for the following range: deuteron energy from 100 Kev to 25 Mev and at angles 0, 5, 10, 15, 20 degrees and until 180 by step of 10.

In fig. 3, the neutron energies as a function of bombarding energy is shown for neutrons emitted at various angles in the laboratory system of coordinate. Curves of fig. 4 show how to cover most efficiently the complete range of neutron energies by using the proper angle.

The solid angle subtended at the chamber is governed by the neutron energy spread permissible (in this work, ± 10 Kev). As shown in fig. 3, $\frac{\Delta En}{\Delta\theta}$ is minimum at zero degree, there-

fore all the runs were done at 0 degree. The table below shows the position of the chamber (distances and angles) used to cover the complete neutron energy range.

Neutron energy, (Mev)	Angle (degree)	Distance "d" (cm)
$E_n > 4.5$	0	100
$3 < E_n < 4.5$	0	80

3. Beam and Target System

For fast neutron measurements of the type described in this work, there are three main problems. First of all the incident deuteron beam must be made accurately monokinetic if the spread in neutron energy is to be kept small - a figure of less than 25 Kev was the aim in this work. For this purpose accurately adjustable entrance and exit slits were made for the 90° deflecting magnet. Secondly, to avoid spurious monitoring of the neutron flux, it is highly desirable that the vast majority of the neutrons entering the neon chamber and monitor originate in the heavy ice target and not somewhere along the beam path. It is not possible to avoid some neutron production in the magnet box due to the molecular beam component and build up of deuteron on the defining slits. Consequently the heavy ice target was placed a considerable distance (13-1/2 feet) from the magnet box, and an electrostatic quadrupole lens focused the beam through the beam pipe at the target. The third problem is that of scattered neutrons which are degraded in

energy, then pass through either neon-filled chamber or monitors. Collimation schemes are large and costly, and no attempt along these lines was made: the floor being almost 3 feet from the target, the near wall of the room some 8 feet and no other wall close, it was considered adequate to merely keep down the scattering material in the vicinity of the target to a minimum.

The overall system used is shown in fig. 5 and the details of the target pot in fig. 6.

4. Heavy Ice Target

To provide a deuteron target to be bombarded with deuterons, heavy water was frozen onto a metal plate refrigerated with liquid nitrogen. The quantity of heavy water sprayed was measured by the so-called D_2O evaporator which has been built for the new D-target pot. The details of the operation and a photograph of a similar device is given on p. 18 and 24 of Larson's thesis (1957). Such a device consists of a liquid D_2O reservoir which is at room temperature and joins to the vacuum system so that on the opening of the valve, D_2O vapor escapes and impinges on the cold plate which serves as a vapor pump.

The target, on which the ice was deposited, was of copper sheet 1/32 inch thick, 1-1/8 by 1-1/4, which has been gold plated. It was fastened tightly to an hollow brass tube containing liquid nitrogen.

The temperature of the ice should be kept below -100°C in order that the target does not vaporize too quickly.

The thermal conductivity of ice at this temperature is only of the order of 0.009 cal./°C-cm-sec. (Fast Neutron Physics, Chap. IV, by J. H. Coon).

Chapter III

MONITOR OF THE NEUTRON FLUX

The neutron flux incident upon the neon-filled chamber was monitored by means of a "long counter" (or boron trifluoride counter) and a "lucite zinc sulphide counter, and was also measured by means of the current integrator.

The current integrator measures the quantity of charge from the deuteron beam hitting the target and if the number of target deuterons per sq. cm. is known, the neutron yield is then obtained from the cross section data, as given in the review article of Fowler and Brolley (1956).

The lucite zinc sulphide counter is a gamma-ray insensitive fast neutron counter, (Griffiths et al, Can. J. of Phys., Vol. 37, 1959). It consists of rectangular sheets of lucite coated with zinc sulphide sandwiched together and mounted on a photomultiplier tube (RCA 6342). The discriminator may be chosen so that it counts mostly neutrons of a certain minimum energy. The absolute efficiency, defined as the number of counts observed divided by the number of neutrons incident on the front face of the counter, is, of course, a function of the discriminator level. For this work, the discrimination level was set at 450 (pulse height) which corresponded to an efficiency of 0.3% for neutron energy of about 5 Mev; see fig. 5 and 6 of the above mentioned article for the efficiency at different neutron energy.

The "long counter" due to its geometry (longer than its

mean free path of the highest neutron energy to be counted) has the same efficiency for neutrons of all energies above a few hundred Kev. Most neutrons entering the inner cylinder of paraffin are thermalized by collision with protons and drift into the counter where they produce pulses through $B^{10}(n, \alpha)Li^{7}$ reaction. The detecting efficiency of this counter was determined by placing a calibrated Ra-Be source (51 millicuries) at the position normally occupied by the D-target. The monitor gives 4.6 counts for every 10^{6} neutrons emitted by the source at the position on its axis 150 cm from its face which corresponds to an efficiency of 0.45%. The actual counter used for the work is fully described by Heiberg (1954). The experimental arrangement is shown in fig. 5.

Chapter IV

Possible Reactions

Since neon contains three isotopes, Ne^{20}, Ne^{21} and Ne^{22}, a number of fast neutron induced reactions resulting in charged particles are possible. Then permitted by the Q-value, incident neutron energy together with the elastic neon recoils will give rise to the pulse height distribution observed. The table below sets out the possible reactions together with their Q-values, which have been taken from the preprint of Rev. Mod. Phys. (Ajzenberg and Lauritsen, 1960), except the one with an asterisk which has been calculated using the empirical mass formula for F^{22}.

Isotope	Abundance	Reaction	Q-value (Mev)
Ne^{20}	90.22%	$Ne^{20}(n,\alpha)O^{17}$	-0.608
		$Ne^{20}(n,p)F^{20}$	-6.267
Ne^{21}	0.26%	$Ne^{21}(n,\alpha)O^{18}$	+0.704
		$Ne^{21}(n,p)F^{21}$	-4.945
Ne^{22}	8.82%	$Ne^{22}(n,\alpha)O^{19}$	-5.704
		$Ne^{22}(n,p)F^{22}$	-6*

There may of course also be reactions involving impurities, e.g. $N^{14}(n,p)C^{14}$ which has a large yield: however the gas purity quoted by the manufacturer (maximum limit of possible impurity is: oxygen, hydrogen, nitrogen and helium 0.0005, 0.0005, 0.01 and 0.03 mole percent respectively) together with the filling method (passing through a liquid

nitrogen trap) plus the hot calcium purifier would it is believed preclude this.

Thus for neutrons of energy less than 5 Mev only (n,α) reactions would be expected, and this predominantly from the Ne^{20} isotope. The range of the emitted alpha particle of 5 Mev energy in neon at 8 atmosphere will be about 1 cm. Consequently in this large chamber, the "wall effect" or the number of events arising in which the alphas hit the wall before expending their full energy in ionizing events is quite small of the order of 5% at 5 Mev α-particle. See Appendix "C" for this computation. The maximum kinetic energy imparted to neon nuclei in elastic collision with 5 Mev neutrons will be 1/20 of 5 Mev, or 250 kev and their events would be expected to show as a rise in the count rate at the low pulse amplitude end of the spectrum.

Energy Resolution of the Chamber

Using the 5.15-Mev alpha-particles from a plutonium source, the energy resolution of the chamber has been estimated to be less than 3%. Fig. 9 shows a typical pulse-height distribution where the energy resolution is 2.7%.

The width of the alpha peak is due mainly to the electronic noise and to a smaller degree to the relative position of the ionization event and to the channel width of the kicksorter. However in the present experiment, it is only of importance that the peaks in the distribution curves be resolved.

Energy Measurement of Ionization Events

In the measurement of the energy of α-particle, one relies solely on the ionization chamber as a device giving a linear relation between the energy of ionization and pulse amplitude, and the kicksorter as another device registering the maximum amplitude of those pulses independently of their rise time which may vary due to the different orientation of the ionizing particle.

The 100 channel kicksorter relies for its operation on charging a capacitor through a diode and has a "reading" time between 3.5 and 5 μsec. Then if the rise time is longer than this period, the pulse has not reached its full amplitude at which the kicksorter becomes dead to further input pulses resulting in an apparent loss of gain and decrease in resolution. Therefore the kicksorter was modified to accept pulses 10 μsec wide. A 0.002 μf condensor was put in parallel with the 0.001 μf (catalogue number C-49, from Encoder part), and in order to reduce oscillation a 210Ω resistance was added in series with 0.002 μf condensor. This change permitted a "reading" time up to 10 μsec. Fig. 10 shows the variation in the resolution before and after the modification.

Chapter V

PROCEDURE AND EXPERIMENTAL SET-UP

As mentioned previously the experimental arrangement was chosen to give a very monoenergetic neutron beam with an energy spread of not more than 25 Kev, and at the same time reasonable freedom from fast background neutrons, together with a relatively rapid count rate and hence short running time for any particular run in order to achieve good stability.

The complete experimental arrangement is shown on fig. 5, and the electronics on fig. 7.

The energy of the incoming deuterons was varied from 300 Kev to 2.3 Mev and was measured by the generating voltmeter. The deuteron energies were not taken with continuously increasing energies, but in varying order. Some 5 to 8 runs were taken grouped near data being taken at a "standard" point, in order to check this standard energy at intervals to verify that the heavy ice remained constant. About 5 such standard points were used in covering the complete neutron energy range. After about 8 hours of running, the number of neutrons registered by the neutron monitor was decreased by roughly 15%, presumably due to the ice deterioration.

The quadruple electrostatic lens which focussed the

beam onto the target had to be refocussed when the deuteron energy was changed by more than 200 Kev.

To match readings from day to day, the same series of neutron energies (or "standard" point) was run over, and the kicksorter counts as well as the neutron monitors (which should be consistent) gave the relative neutron yields, and hence relative target thickness.

The ZnS scintillation counter was found to be consistent with the integrator current. However, the BF_3 counter, due to its sensibly flat response to neutrons of all energies above 500 kev, was detecting all neutrons generated both by the desire reaction incident directly and scattered by the floor, walls, etc., into the counter, and by any (d,n) reactions in various parts of the machine. In fact, it was dependent on the time needed for a run and on the exact focussing conditions of the generator, and its reading presumably depended on the D + D build up on the magnet box, etc.

The ZnS counter was placed at a distance of 25 cm from the center of the D-target (measured from the front of the counter) and at right angles with the incident beam. On the other hand, the "long counter" was opposite to the ZnS counter, but at 150 cm from the D-target.

The beam current at maximum energy was kept at about 1 μamp and was proportionally increased by 4 μamp at 300 Kev; at least 50% of the beam going downward was obtained

after 90 degree deflection by the analyzing magnet.

The aperture of the exit and entrance slits was of the order of 1 mm and 2 to 3 mm respectively, With such a setting, a beam of 8 μamp was obtainable at the target. In order to reduce the fringing field at the exit which tended to send the beam in an upward direction, a soft iron pipe 4 inches long and 1/4 of an inch wall thickness was placed as close as possible to the analyzing magnet, immediately after the exit slit.

The beam, after passing through the analyzing magnet, was stabilized by the beam "sniffer"(which provided control of the energy by means of the reverse electron gun), and then focussed at the target by means of the strong focussing electrostatic lens. This lens was at a distance of 6-1/2 feet from the magnet box, and 7 feet from the D-target. The beam before reaching the target, was made to pass through a 6 inch length of 1-1/8 inch diameter copper pipe cooled by a liquid nitrogen trap in order to protect the target from any contamination of carbon which might come from the diffusion pumps. The potential on the focussing lens was adjusted by varying the voltage on each lens until the light spot made by the beam hitting the quartz focussing plate (which is 3 inches ahead of the target) was as small a spot as possible. The plate was then removed, allowing the beam to lead to the target. The beam at the target was intentionally unfocussed so that the spot appeared as a circle of about 1/8 of an

inch in diameter rather than a point to prevent evaporation of the ice by spot. The target itself was kept at a potential of +90 volts to eliminate the effect of secondary electrons ejected from the target on the target current-recorded.

The D_2O targets were made by condensing heavy water vapor from a constant volume dispenser onto a liquid air cooled gold plate. The dispenser-target system was calibrated by observing the shift in the 873-Kev resonance of the $F^{19}(p, \alpha, \gamma)O^{16}$ reaction after a pressure of 6 cm of oil of D_2O vapor was deposited on a thin calcium fluoride target.

The Van de Graaff generating voltmeter was calibrated using the accurately known resonances of the $F^{19}(p, \alpha, \gamma)O^{16}$ reaction, and it was found that the generating voltmeter was reading the correct voltage within 1/2%. Fig. 8 shows one of the calibration point at 873-Kev energy.

The center of the chamber was placed at a distance "d" (measured from the D-target) which was governed by the solid angle required to keep the energy spread of the neutron beam within $\pm$10 Kev. The following table shows the distance and the angles used to cover the range of neutron energy desired.

Neutron energy (Mev)	Angle (degree)	Distance "d" (cm)
$En > 4.5$	0	100
$3 < En < 4.5$	0	80

In order to reduce the neutron background going into the chamber and into the monitor, a wall of wax (9 inches thick) was built between the quadrupole lens and the D-target. Nevertheless it made no significant improvement.

The total neutron energy spread was kept lower than 25 Kev, except below 3.7 Mev where it goes up to 40 Kev. The total neutron energy spread, ΔE_n, is calculated by the equation

$$\Delta E_n = \sqrt{\Delta E_n\ (\Delta E_d)^2 + \Delta E_n(\theta)^2 + \Delta E_n(tg)^2}$$

where ΔE_n is the total neutron energy spread

$\Delta E_n(\Delta E_d)$ is the variation of the neutron energy due to the variation of energy in the deuteron beam (assume $\Delta E_d = \pm 5$ Kev)

$\Delta E_n(\theta)$ is the neutron energy spread due to the angular distribution of the outgoing neutrons from the D on D reaction

$\Delta E_n(tg)$ is the target thickness in neutron energy

Neutron Energy Mev	Distance d,(cm)	$\Delta E_n(\Delta E_d)$ Kev	$\Delta E_n(\theta)$ Kev	$\Delta E_n(tg)$ Kev	ΔE_n Kev
3.500	150	14	32	2.3	35
4.244	100	11.5	16.5	6.1	21
5.500	100	10.5	9	12	18

The preceding table is a typical estimate of the neutron energy spread at three different energies.

Chapter VI

DETERMINATION OF THE ABSOLUTE CROSS SECTION

1. General Expression for the Cross Section

The general expression for the total number of disintegration events in the chamber is given by

$$N_r = \int_{\Omega} N_n \, \sigma(E) \, \eta(d\Omega) \, d\Omega \qquad (1)$$

where: N_r is the number of neon disintegrations registered by the kicksorter per count on the current integrator (one integrator count corresponds to an integrated beam current of 95.0 ± 0.5 μcoulombs).

N_n is the number of neutrons produced by $D(d,n)He^3$ reaction in the element of solid angle $d\Omega$ per integrator count and per steradian, of energy E.

$\sigma(E)$ is the total cross section of the reaction in cm^2, at neutron energy E.

$\eta(d\Omega)$ is the areal density of neon atoms in the element of solid angle $d\Omega$, (atoms/cm^2).

Ω is the solid angle in steradian subtended at the target by the chamber.

If q is the quantity of charge carried by the deuteron beam (in μcoulomb per integrator) measured by the current integrator and hence is a measure of the number of incident deuterons, then N_n may be written

$$N_n \text{ in } d\Omega = K\ n_D\ q\ \sigma_D(E_D, \theta)$$

where: K is a proportionality constant equal to 6.25×10^{12} electronic charges per μcoulomb ($10^{-6} \frac{\text{coul.}}{\mu\text{coul.}} \times \frac{1}{1.6\times10^{-19}} \frac{\text{esu}}{\text{coul.}}$)

n_D is the number of D-atoms in the target per cm^2.

$\sigma(E, \theta)$ is the differential cross section of the $D(d,n)He^3$ reaction in cm^2 per steradian.

Since the solid angle subtended by the chamber was made small (less than 0.034 steradians) and the cross section in this interval may be assumed constant, thus the equation (1) becomes

$$N_r = K\ q\ n_D\ \sigma_D(E_D, \theta)\ \sigma(E) \int_\Omega \eta(d\Omega)\ d\Omega \qquad (3)$$

the above integral is by definition equal to

$$\int_\Omega \eta(d\Omega)\ d\Omega = \bar{\eta}\,\Omega \qquad (4)$$

where $\bar{\eta}$ is the average areal density of neon atoms, (atoms/cm^2).

If one averages using small elements of solid angle, the computation is quite tedious. But, since the chamber subtends a small solid angle, one can consider as a good approximation the incoming neutrons as a parallel beam as shown in fig. 11. This assumption really leads to an error

not too large in correct choice of d^2, i.e. one really would have to weigh the elements as $1/R^2$ and get a mean value.

From equation (4)

$$\bar{\eta} = \frac{\int_\Omega \eta(d\Omega)\, d\Omega}{\int_\Omega d\Omega}$$

Due to the above assumption (the incoming neutron being parallel), one can write

$$= \frac{\int_o^R \eta(x)\, dx}{\int_o^R dx}$$

Make the following change of variables:

$$\eta(x) = \rho\, y \qquad \text{and} \qquad y = 2R \sin\theta$$

$$x = R\cos\theta$$

$$dx = -R\sin\theta\, d\theta$$

$$\bar{\eta} = \frac{-2\rho R^2 \int_{\pi/2}^{o} \sin^2\theta\, d\theta}{-R\int_{\pi/2}^{o} \sin\theta\, d\theta}$$

$$= \frac{2\rho R \left[\frac{1}{2}\theta - \frac{1}{4}\sin 2\theta\right]_o^{\pi/2}}{\left[-\cos\theta\right]_o^{\pi/2}}$$

$$\bar{\eta} = \frac{\pi}{2}\rho R \quad \text{where } \rho \text{ is the volume density in atoms/cm}^3$$

Now if P denotes the number of atoms, and H, the height

in the sensitive volume of the chamber, one can then write

$$P = \pi R^2 H \rho$$

Since

$$\eta = \frac{\pi}{2} \rho R = \frac{(\pi R^2 H \rho)}{2RH}$$

$$= \frac{P}{A}$$

where A stands for the crossectional area of the chamber. Hence

$$P = A \bar{\eta}$$

and the solid angle subtended at the chamber is

$$\Omega = \frac{A}{d^2} \quad \text{(steradian)}$$

It follows that

$$\bar{\eta} \Omega = \frac{P}{d^2} \tag{5}$$

where d is the distance measured from the D-target to the center of the neon-filled chamber.

Equation (4) then becomes

$$N_r = 6.25\ 10^{12}\ q\ n_D\ \sigma_D(E_D,\theta)\ \sigma(E)\ \frac{P}{d^2} \tag{6}$$

2. Correction for absorption of the incident neutron beam passing through the chamber wall

From the total number of neutrons emitted into the solid angle of the chamber, a certain fraction may be absorbed or scattered by the steel wall of the chamber

pressure vessel so that they do not contribute to the disintegrations at the energy considered. If one considers the attenuation occurring in the steel of the chamber closest the neutron source, then one can estimate the fraction ζ of neutrons which contribute to the reaction using the usual absorption equation

$$R = R_o e^{-\mu x}$$

where: R_o is the number of incoming neutrons

R is the number of neutrons traversing the iron wall of the chamber

μ is the linear absorption coefficient = $n_a \sigma_a$

x is the average thickness of the absorber ($\approx 1/8"$)

n_a is the number of atoms in the absorber/cm^3

σ_a is the total neutron cross section of iron (3.7 barns at about 5-Mev neutron energy, obtained from Hughes and Schwartz (BNL-325), 1958

$$n_a = \frac{N_o \rho}{W} = 8.4 \times 10^{22} \text{ iron atoms/cm}^3$$

and $$\mu = n_a \sigma_a = 0.31 \text{ cm}^{-1}$$

where N_o is the Avogadro's number, 6.02×10^{23}

ρ is the density, 7.8 gm/cm^3

W is the atomic weight (for iron 56: its most abundant isotope is Fe^{56}, 92%)

Finally,

$$\zeta = \frac{R}{R_o} = 0.91$$

3. Determination of the number of deuteron atoms per cm^2 in the D_2O target

The number of deuteron atoms per square cm at the target is determined by the knowledge of the stopping cross section.

$$\epsilon(E) = \frac{1}{n_D'} \frac{dE}{dx}$$

$$\text{or} \qquad \epsilon(E) = \frac{T \times 10^3 \times 2}{n_D}$$

where $\epsilon(E)$ is the molecular stopping cross section in ev.-cm^2 at energy E.- For D_2O and H_2O, see fig. 12.

$\frac{dE}{dx}$ is the loss of energy per unit path length in ev./cm.

T is the target thickness in Kev. See appendix B for the experimental measurement.

n_D' is the number of molecules of D_2O per cm^3.

n_D is the number of atoms of deuterium per cm^2.

Note that the factor 2 transforms molecules into atoms. As an example, a target thickness of 11 Kev was achieved by evaporating 6 cms of oil pressure of D_2O vapor from the

evaporator, which correspond to 2.62×10^{18} atoms of deuteron per cm^2.

4. Determination of the number of neon atoms in the sensitive volume of the chamber

The number of neon atoms "P" in the sensitive volume of the chamber is estimated by knowing the pressure (8.1 atm.) of the neon in the chamber and its sensitive volume. The sensitive volume of the chamber is 4.11 liters calculated by

$$V = \frac{\pi}{4} (D^2 - d^2)H$$

where D is the inside diameter of the chamber (6")
d is the diameter of the gridded region of the chamber (11/16")
H is the length of the gridded region of the chamber (8-7/8")

Then the number of neon atoms P, contained in the sensitive volume of the chamber is calculated by the formula

$$p\,V = \frac{P}{N_o} RT$$

where R is the gas constant
T is (273 + 23) °K
N_o is Avogadro number, 6.02×10^{23}

Hence the number of atoms, P, is equal to 8.26×10^{23}.

5. Typical calculation of the absolute cross section

As an example, take the calculation of the cross section for the ground state alpha-group at 1250-Kev deuteron energy. The chamber was at 100 cms from the neutron source and was making an angle of zero degrees with respect to the accelerated beam. Six cms of oil pressure gave a target measured as having a thickness, T, equal to 11 Kev to protons of 873 Kev. This corresponds to a thickness of 12.9 Kev to deuteron of 1250-Kev. The molecular stopping cross section of heavy water at this energy is 10.7×10^{-15} ev.-cm^2, hence the number of D-atoms per square centimeter, n_D is 2.62×10^{18}.

From the following data

$N_r = \frac{2470}{5}$ disintegrations per integrator

$d = 100$ cms

$q = 95 \times 10^{-6}$ coulombs/integrator

$\sigma_D(E_D\theta) = 31.7$ mb or 31.7×10^{-27} cm^2

substituting into equation (6), the total cross section $\sigma(E)$ for the reaction $Ne^{20}(n,\alpha)O^{17}$ is found to be 133 mb:

$$\frac{2470}{5} = 6.25 \times 10^{12} \frac{1}{0.91} \times 95 \times (2.62 \times 10^{18})\ (31.7 \times 10^{-27})\ \sigma(E)(\text{mb}) \times 10^{-27} \times \frac{8.26 \times 10^{23}}{(100)^2}$$

hence $\sigma(E) = 133$ mb.

Similar calculation for the cross section was made at various neutron energies and their respective cross section is given below. Table 1 gives some details of this calculation.

Neutron Energy in Mev	for Ne(n, α) in mb
3.418	183
3.793	285
4.033	198
4.234	128
4.386	136
4.841	92

The cross section curve after normalization was made to pass through those points by making a linear correction between each pair of points. The correction (or shift) was less than 10%, except between 3.8 and 4.05 Mev where the correction went up to 30%.

Table 1

En (Mev)	Run No.	No. of Counts	No. of Integrators	Dist. cm	$\sigma_D(E_D 0°)$ (mb)	D_2O cm of Oil	Ne (mb)	Ne (Weighted) (mb)
3.418	H-5	856	5	100	9	4.9	183	183
3.793	H-4	2238	5	100	16.5	4.9	296	285
	H-6	2099				4.9	277	
	J-4	2279				4.9	301	
	J-4'	2009				4.9	266	
4.033	H-3	2117	5	100	22.2	4.9	208	198
	H-7	1978				4.9	194	
	J-3	1991				4.9	196	
	J-3'	2043				5.0	194	
4.234	H-1	1674	5	100	28.5	4.9	128	128
	H-9	1729				4.9	132	
	J-2	1793				4.9	137	
	J-7	1627				4.9	124	
	J-11	1556				4.9	119	
	L-1,4	1625				5.0	120	
4.386	H-10	1897	5	100	31.7	4.9	130	136
	J-8	1842				4.9	127	
	J-10	2012				4.9	138	
	L-5,17	2072				5.0	138	
4,841	J-9	2381	5	100	38.5	4.9	134	92
	H-11	1859				4.9	105	
	L-6	1647				4.9	89	
	L-7	1580				5.0	86	

Chapter VII

RESULTS

In most of the neutron energy range used (3.2 to 5.5 Mev), two distinct disintegration peaks appeared in the pulse-height distribution which were due to two different disintegration groups, $Ne^{20}(n,\alpha)O^{17}$ and $Ne^{20}(n,\alpha)O^{17*}$. The transition to the ground state and to the first excited level are labelled respectively "long" and "short" range α-particles. From the pulse-height distribution curves taken at small energy interval (12-kev deuteron energy), the Q-values of disintegrations and the excitation function of the compound nucleus, Ne^{21}, formed was determined. Also knowing the target thickness, the absolute cross section has been estimated.

1. Q-values

The energy released in the disintegration was obtained by subtracting the total energy of ionization from the energy of the incident neutron. The neutron energies were found from the energies of the incoming deuteron beam reduced by the mean value of the beam energy lost in going through the heavy ice target. The neutron energies in function of the deuteron energies were obtained from published tables (Fowler and Brolley, 1955). The total energy of ionization was determined from the relative position of the peak on the kicksorter, having previously calibrated

the channel number in function of energy using as reference the 5.15 Mev Pu-α source. Typical curves, from which Q-values were found, are shown in fig. 13, for various neutron energies.

The Q-values for about thirty peaks (for each of the two cases: Q_1 and Q_2 defined below) were calculated and then averaged. Q_1 corresponds to the ground state transition $Ne^{20}(n,\alpha)O^{17}$, and Q_2 corresponds to the transition $Ne^{20}(n,\alpha)O^{17*}$, where O^{17*} is left in its first excited state.

The final Q-values obtained are -0.69, $\pm$0.02 Mev and -1.57 $\pm$ 0.02 Mev for the reaction $Ne^{20}(n,\alpha)O^{17}$ and $Ne^{20}(n,\alpha)O^{17*}$ respectively. The errors quoted are the r.m.s. errors.

2. Excitation Function

The excitation function in the neutron energy range from 3.2 to 5.5 Mev was found from three sets of runs based on reference energies of 0.460, 0.740, 0.930, 1.100, 1.230, 1.600 and 1.800 Mev. The number of disintegrations associated with each particle group was calculated from the pulse-height distribution similar to those shown in fig. 13. For the full energy peak, the number of disintegrationsis taken as the integrated number of counts under the peak reduced by the background which was taken as having an area corresponding to one half the height of the knee at the lower end of the peak (the ratio of this area over the total area under the peak was of the order of 5%, i.e. ranging from 3% to 7%).

These numbers were then normalized to correspond to the same distance from the target (100 cm), and the same number of integrators. Two curves were then drawn. The first one was normalized as mentioned above, and represented a plot of the yield against energy using the integrated deuteron beam as a measure of the incident neutron flux. The second was normalized to the same number of counts of the zinc sulphide neutron monitor. This neutron counter has an efficiency which increases slowly and monotonically with the neutron energy, so that for a small energy range, its efficiency is approximately constant. Those two curves were used concurrently in order to eliminate any erroneous point which can be found by comparing point by point those two curves. The zinc sulphide counter thus provided a check on target deterioration and change but was itself susceptible to beam wandering, as part of its reading come from background neutrons.

A supplementary series of points were taken in the neutron energy range from 4.4 to 4.8 Mev, because of a discrepancy noticedin the number of disintegrations when running over this region with decreasing the energy. Although all this care was taken, the matching of those three curves were not as good as expected; so additional runs were performed.

In a further attempt to match these three segments of curve, a series of runs covering the complete energy region were done which permitted the normalization of the complete

energy region. These points are shown in red in Plate 1. After this adjustment, the excitation functions for the two groups of α-particles are shown in Plates 1 and 2.

The maxima appear at neutron energy as tabulated below.

Neutron Energies in Mev

Long Range-α	Short Range-α
3.278	---
3.438	---
3.559	3.567
3.708	3.700
3.871	3.874
4.142	4.168
4.304	---
---	4.365
4.575	4.552
4.685	---
---	4.723
4.876	---
4.999	5.016
5.120	
5.203	
5.295	
5.478	

No attempt was made to separate components of peaks such as the one near 4.6, 4.7, 4.9 and 5.0 Mev, because the effect of the "wings" of the other nearby resonances are too large to get a meaningful extrapolation.

3. Absolute Cross Section

In an attempt to determine the absolute cross section, a special series of runs (four independent determinations) were performed in which the current integrator device was carefully calibrated and the target thickness measured.

Using equation (6), page 29, the absolute total cross section was evaluated at neutron energies 3.453, 3.820, 4.052, 4.251, 4,400 and 4,800 Mev. For the details of the calculations and the approximations behind equation (6), see Chapter VI.

Plates 1 and 2 show the excitation function where the ordinate is given in millibarns.

In the determination of the cross section, there are a number of measurements, calculations and corrections which contribute to the error:

1. The integration of each of the two α-groups as obtained from the pulse-height distribution at each neutron energy. An error of about 17% can be allowed due to the reduction of background counts under the peaks.
2. The calculation of the neutron flux from the D on D reaction (error of about 7%), the target thickness and the stopping power in heavy water (error of the order of 10%).
3. The attenuation of the neutrons by the pressure vessel of the chamber (about 2%).
4. The precision of the current integrator device. (Over the complete period of these runs, the variation was less than 1%.)
5. The volume of the sensitive volume of the chamber (about 3% due to the possible error in the dimension of the grid and of the inside diameter of the cylinder).

6. The measurement of the distance of the chamber. (It follows the inverse square law correction; the error is less than 1%.)
7. The measurement of the gas pressure in the chamber. (Error of 1%, due to the precision of the pressure gauge.)
8. The correction for the wall effect. As calculated in Appendix C, the number of disintegrations falling outside the peak is less than 5% at energy below 5-Mev α-particle.
9. The counting statistics. The error goes up to 3% (when the number of counts under the peak is of the order of 1500).

Of these sources of errors, item 1 is the most important. Because the above errors are relatively large compared to the wall effect, the correction for wall effect was not made.

Based on the above considerations, estimates of the probable errors in the determination of the cross section is about $\pm$ 20%. Relative error in the data are somewhat less than these absolute error estimates. This is an optimistic estimate, since they may be hidden systematic errors.

4. Special Run at 16.7 Mev Neutron Energy

A special energy spectrum was taken at 16.74 neutron energy using $D(T,n)He^4$ as source of neutrons; the target

thickness was about 75 kev. At this energy, the complete energy spectrum with several peaks corresponding to various energies dissipated in the chamber is shown in Plate 3.

Maxima in the energy distribution appear at 3.05, 3.9, 4.25, 5.8, 8.3, 10.0 and 12.7 Mev, a very wide peak between 15 and 16.5 Mev, and a shoulder between 2 and 3 Mev.

The 10-Mev peak is probably due to the reaction $Ne^{20}(n,p)F^{20}$ where the fluorine is left in its ground state; this is on the basis of a correct calculated Q-value from masses.

The broad peak between 15 and 16.5 Mev is probably due to the $Ne^{20}(n,\alpha)O^{17}$ and O^{17*} reactions, leaving O^{17} in its ground state and in its first excited state. Also the 12.8 Mev peak is due to the same reaction, but leaving the O^{17} in its second excited state.

The shoulder between 2 and 3 Mev may be explained by the neon recoils arising from neutrons elastically scattered. From collision theory, it has been calculated that, for an elastic collision, the neon nucleus can carry up to 3.03 Mev.

Coming back to the range 15 to 16.5 Mev, the smear out in this region, where the reaction $Ne^{20}(n,\alpha)O^{17}$ is going to the ground state and to the first excited state of O^{17}, may be attributed to the ionizing effect of the recoil nucleus being a little different from that of an α-particle. This will have the effect of spreading the peak.

DISCUSSION OF RESULTS

1. Q-values

In the energy spectrums, below neutron energy of 5.5 Mev, only two peaks appear and from their Q-values (Q_1 and Q_2) there is no doubt that they correspond to the reactions $Ne^{20}(n,\alpha)O^{17}$ and $Ne^{20}(n,\alpha)O^{17*}$ where O^{17*} stands for the first excited level of O^{17}.

Then a precise measurement of Q_1 and Q_2 were taken on thirty different energy spectrums, chosen in the neutron energy range of 3.2 to 5.5 Mev. The measurement of Q_1 is in agreement with the result of Flack (-0.70 ± 0.05). Also the excited state of O^{17} lies at 0.88 ± 0.01 Mev above the ground state in agreement with the value of 0.872 Mev quoted by Ajzenberg and Lauritsen (1955).

In the energy spectrum obtained at 16.74-Mev neutron energy, the 10-Mev peak was identified as being due to the $Ne^{20}(n,p)F^{20}$ reaction when the F^{20} is left in its ground state. The Q-value of this reaction has been measured to be -6.1 ± 0.2 Mev compared with -6.267 Mev calculated from the masses (Ajzenberg and Lauritsen, 1955).

2. Excitation function

The results of Bonner et al (1959) and those of Flack (1952) are given in Table 2. Considering only the (n,α) process leaving O^{17} in its ground state, then maxima in this work appear mostly in accord with their results. All

maxima observed by Bonner have also been observed here, except at 3.559 Mev where he found two peaks at 3.52 and 3.60 Mev.

Most resonances in both α-particle groups led to the same excitation energy of the compound nucleus, Ne^{20}, as expected by the theory.

Table 2

Excitation Energy of Ne^{21} (Mev)	Neutron Energy at Maxima in Mev				
	1st α-group		2nd α-group	Bonner	Flack
		Width Kev			
10.035	3.278	70		3.29	3.24
10.195	3.438	65*			3.48
10.316	3.559	70*	3.567	(3.52 (3.60	
10.465	3.708	110	3.700	3.70	3.74
10.628	3.871	110	3.874	3.87	3.91
10.899	4.142	80	4.168	4.15	4.15
11.061	4.304	55		4.31	4.30
			4.365		4.50
11.332	4.575	80*	4.552		4.58
11.442	4.685	100*		4.62	4.65
			4.723		4.74
11.633	4.876	60*			4.85
11.756	4.999	90	5.016	4.98	4.97
11.877	5.120				
11.960	5.203				
12.052	5.295				
12.235	5.478	120*		5.52	

Assuming the binding energy of a neutron in Ne^{20} lies 6.756 Mev (Ajzenberg and Lauritsen, 1959) above the ground state, then the energy levels in Ne^{21} corresponding to these resonances lie between excitation energies of 10.035

and 12.235 Mev (Table 2). But the uncertainty in the neutron energy was kept below 25 Kev, except below 3.7 Mev where it goes up to 40 Kev. Therefore, the energies at which maxima are judged to occur are of about the same accuracy.

Since the reaction widths are wider than the neutron width (i.e. neutron energy spread) one can believe that the measured widths are in fact a direct measure of the natural width of these levels. The measured reaction widths are given in Table 2, where * indicates that one has resolved graphically the peak and then estimated the width.

3. Absolute Cross Section

The values of the cross section quoted by Flack (1952), using a gridded parallel plate ionization chamber, are between 2.5 and 12.5 mb (in the range 3.2 to 5.1 Mev, neutron energy) which are in disagreement with the values obtained here by a factor roughly 30 smaller.

Johnson et al (1951), using a proportional counter as a detector, gave a cross section of 160 mb at a neutron energy of 3.26 Mev. This value is a factor 2.5 smaller than the value reported here. However, Bonner et al (1959), using also a gridded parallel plate ionization chamber, found a peak at 3.29 Mev with a corresponding cross section of 210 mb. This value is a factor 1.9 smaller than our value.

Our values of the cross section, which is larger than the values reported by other workers, may be partially due to the better symmetry of our ionization chamber. One might expect that our peaks are less smeared out, and therefore maxima in the excitation curve could be higher. It would be conclusive if the value of the absolute cross section at one energy or two would have been taken by using deuterium gas target.

Nevertheless it is believed that our absolute cross section for $Ne^{20}(n,\alpha)O^{17}$ reaction is accurate to $\pm$ 15%; this value is based on an estimate given on page 40. However the error in the relative cross section is somewhat less.

APPENDIX A

Calculation of the efficiency of the grid and the transparency to electrons

The calculation is quite complicated and has been performed by Bunemann (1949). The result is expressed in terms of parameters in function of the grid constant and the applied voltage on the electrodes.

The inefficiency " σ " of the grid represents the fraction of the lines of force which end on the grid and those which end on the collector. (The word "end" may be replaced by "start" depending on whether the collector is positive or negative.) On the other hand the transparency " λ " to electrons represents the fraction of the electrons collected onto the grid.

From Fig. 3 and 4 of Bunemann's paper, and using his notation, one gets the following results:

Given: $2r = 0.005"$ $\quad V_P = 2{,}500$ volts

$d = 2$ mm $\quad V_G = 1{,}250$ volts

$p = 8.75$ mm $\quad V_A = 0$ volts

$a = 6.75$ mm

Then $\frac{r}{d} = 0.03$ and $\frac{d}{p} = 0.23$; therefore from Fig. 3, $\sigma = 0.06$ and the inefficiency of the grid is then 0.94.

Now $\rho = \frac{2\pi r}{d} = 0.20$ and $\frac{EP}{EQ} = 7.7$: from Fig. 4, $\lambda = 0$. Therefore the fraction of the electron collected is zero.

APPENDIX B

D_2O target thickness measurement

The thickness of the D_2O ice target was measured by observing the shift of the 873-kev resonance of $F^{19}(p,\alpha,\gamma)O^{16}$ reaction after a given quantity of D_2O vapor was deposited on a thin calcium fluoride target. The excitation function for this reaction was determined in the neighborhood of the accurately known 873-kev resonance. The increase in the incident proton energy required to produce resonance, when passing through the ice layer, was considered to be equal to the mean energy lost by the protons in traversing the heavy-ice layer.

It has been shown experimentally and theoretically that the stopping cross section for proton and deuteron of the same velocity are equal. On this basis, the stopping cross section for a given proton energy is the same as for a deuteron of double energy.

In the heavy-ice pot, the gold target was replaced by the thin CaF target. A similar heavy-ice target was laid down on that target. The target was operated at a potential of +90 volts to suppress secondary electrons. With a pressure corresponding to 6 cm of oil, the target turned out to be 11 kev thick (see Fig. 8) at 873-kev proton, or 1746-kev deuteron energy. Using Fig. 12, one finds that the ice thickness is 18-kev at 873-kev deuteron energy.

APPENDIX C

Wall effect correction for cylindrical detector

The wall effect correction is the determination of the fraction of the events not counted in the peak. Some particles will hit the wall during their ionization path and the pulse then produced may have any energy up to the maximum energy of the particle.

Rossi and Staub (1949) have derived an expression and their approximate detection efficiency " ϵ " is given by

$$\epsilon = 1 - \frac{r(B)}{2b}$$

where

b : the radius of the cylindrical chamber (3 inches)

$r(B) = R_o - R(E_o - B)$

R_o : maximum range of the charged particle

$R(E_o-B)$: range of particle at energy E_o-B

E_o : original energy of the particle

B : bias energy

From the range of α-particles and of protons at various energies (Whaling, 1958), the detector efficiency is calculated by the above formula. The results are tabulated in the following table for α-particles from 3 to 15 Mev and for protons up to 10 Mev.

Ionizing Particles	E_o Mev	B Mev	R_o cm	%
Alphas	3	3	0.38	97
	4	4	0.55	96
	5	5	0.75	95
	6	6	1.0	93
	10	10	2.2	86
	15	15	4.24	72
Protons	4	4	4.76	69
		3		72
	6	6	9.45	38
		5		41
	10	4	22.8	16

REFERENCES

Aaronson, D. 1950. M.A. Thesis, U.B.C.

Ajzenberg, F. and Lauritsen, T. 1959. Nuclear Physics, 11, No. 1

Bullock, M. L. 1959. Rev. of Sci. Instr. 30, 251

Bunemann, Cranshaw and Harvey. 1949. Can. J. of Res., A, 27, 191

Courant, Livingston and Snyder. 1952. Phys. Rev. 88, 1190

Enge, H. A. 1959. Rev. of Sci. Instr., 30, 248

Erdman, K. L. 1953. Ph.D. Thesis, U.B.C.

Flack, F. C. 1952. Report on Disintegration of Neon by Fast Neutrons, Unpublished, U.B.C.

Fowler and Brolley, 1956. Rev. Mod. Phys. 28, 126

Frisch, O. R. Unpublished report, BR-49, British Atomic Energy Project

Gabbard, Bell and Bonner. 1959. Am. Phys. Soc., March

Gabbard, Bichsel and Bonner. 1959. Nuclear Physics, 14, No.2

Graves and Coon. 1946. Phys. Rev. 70, 101

Griffiths, Singh, Ssu and Warren. 1959. Can. J. Phys. 37, 858

Gurney. 1925. Proc. Roy. Soc., A, 107, 332

Hanson. 1947. Phys. Rev. 72, 673

Harkins, Gans and Newson. 1935. Phys. Rev. 47, 52

Heiberg. 195 . Ph.D. Thesis, U.B.C.,

Hughes, D. and Schwartz, R. 1958., BNL 325

Johnson, Bockelman and Barschall. 1951. Phys. Rev. 82, 117

Larson, E. 1957. M.A. Thesis, U.B.C.

Marion and Fowler. Fast Neutron Physics

Schnider, K. 1939. Ann. Phys. 35, 445

Sikkema. 1950. Nature, 165, 1016

Stetter, G. 1943. Z.f.Phys. 120, 639

Tollestrup, Jenkins, Fowler and Lauritsen. 1949. Phys. Rev. 76, 181

Warren and Hay. 1959. Can. J. Phys. 37, 1153

Wilkinson, D. H. 1950. Ionization Chambers and Counters, Cambridge University Press

Zagor and Valente. 1945. Phys. Rev. 67, 133

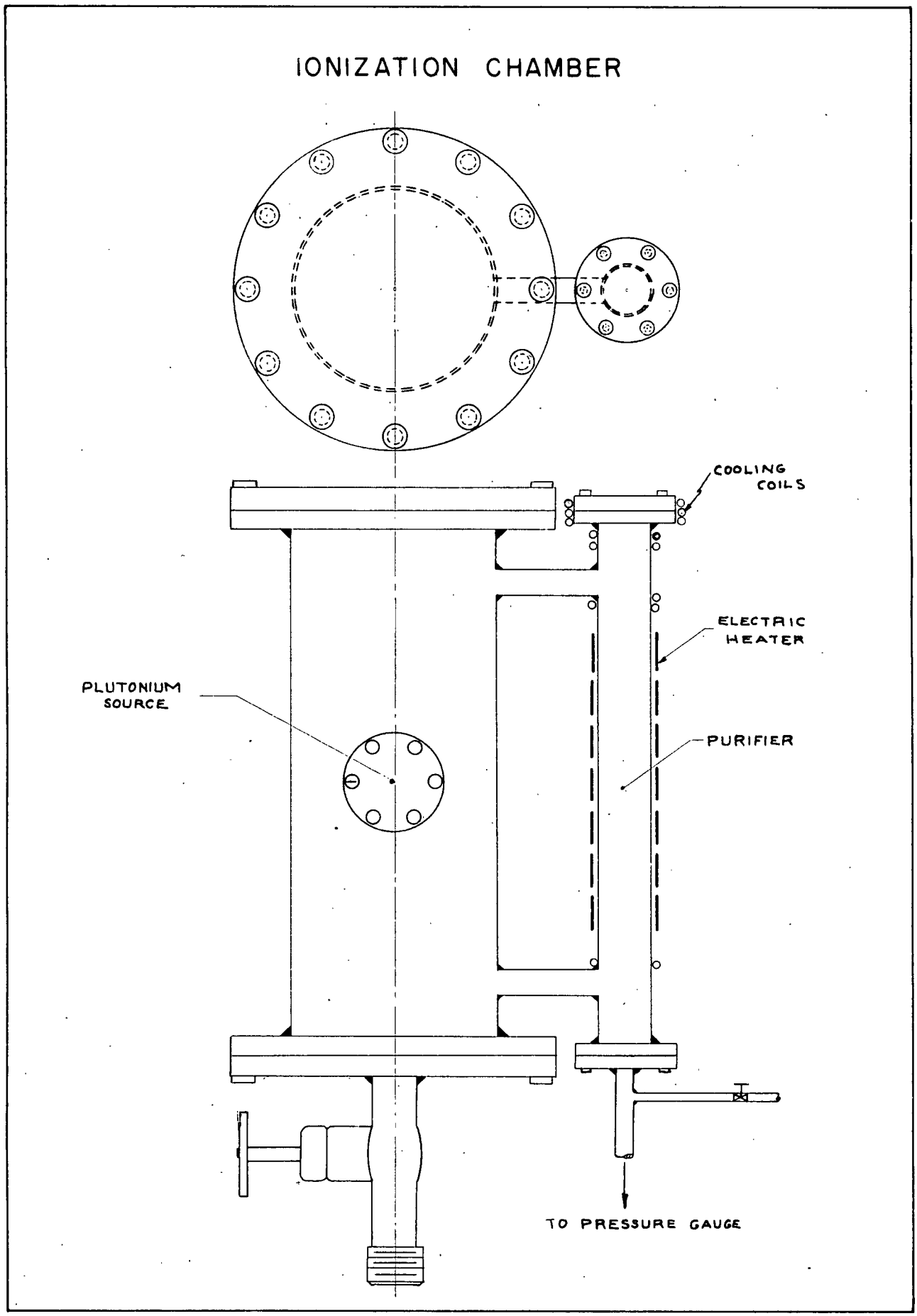
IONIZATION CHAMBER
COOLING COILS
ELECTRIC HEATER
PLUTONIUM SOURCE
PURIFIER
TO PRESSURE GAUGE

FIG. 1

IONIZATION CHAMBER
DETAIL OF THE GRID.

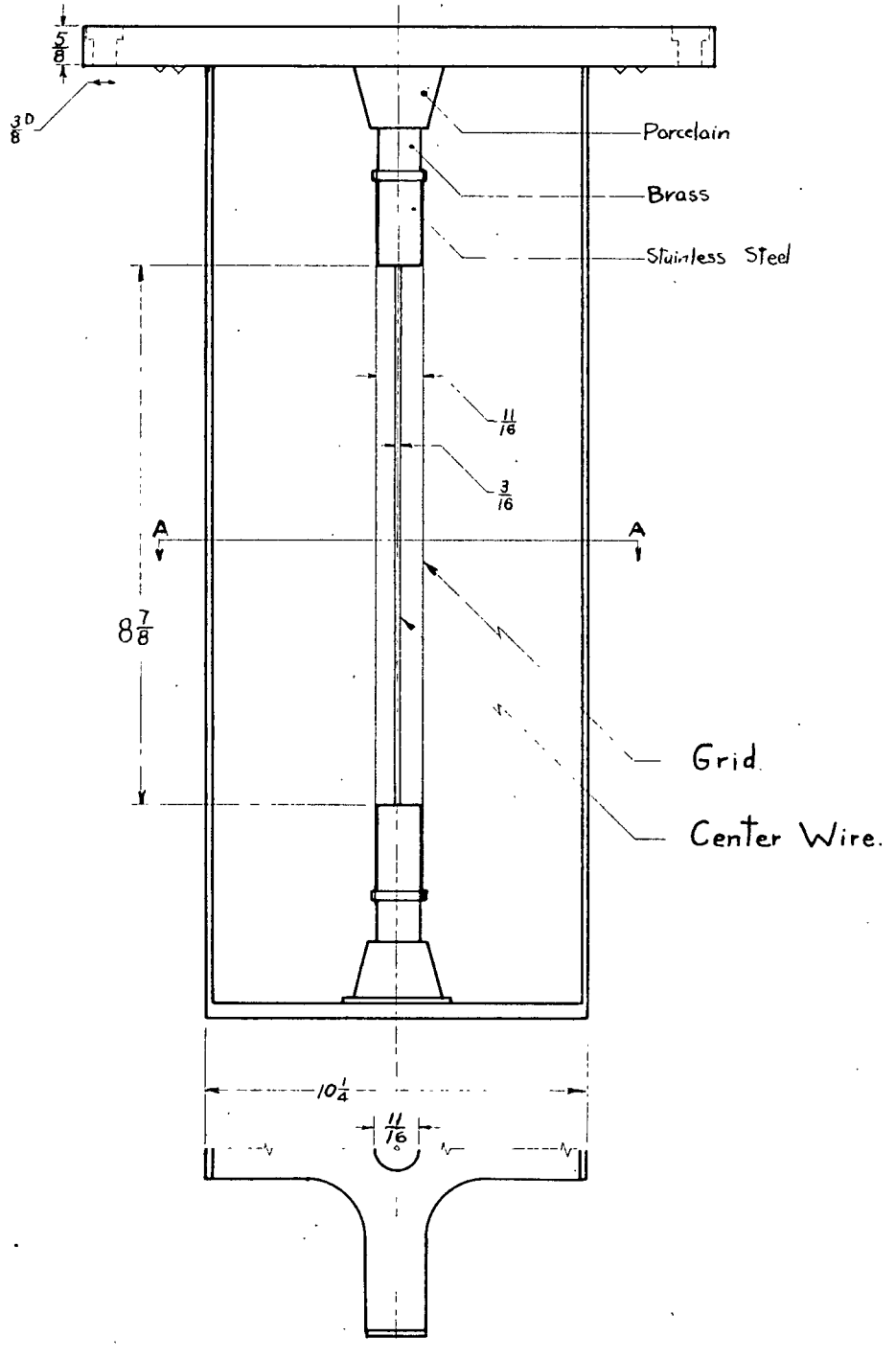

Section A-A

Scale : 1" = 3"

FIG. 2

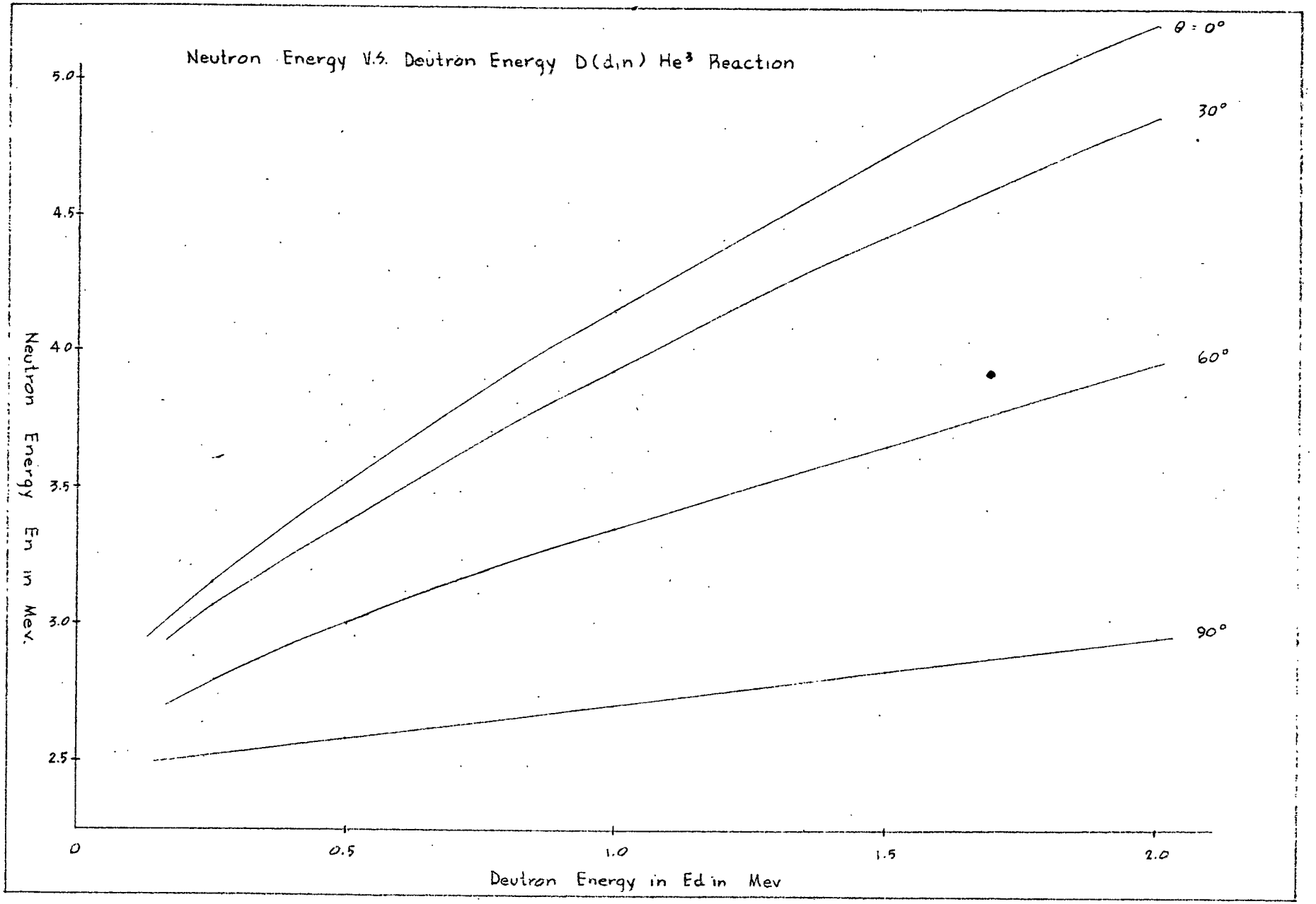
Neutron Energy V.S. Deutron Energy D(d,n) He³ Reaction
θ = 0°
30°
60°
90°
5.0
4.5
4.0
3.5
3.0
2.5
Neutron Energy En in Mev.
0
0.5
1.0
1.5
2.0
Deutron Energy in Ed in Mev

Fig. 3

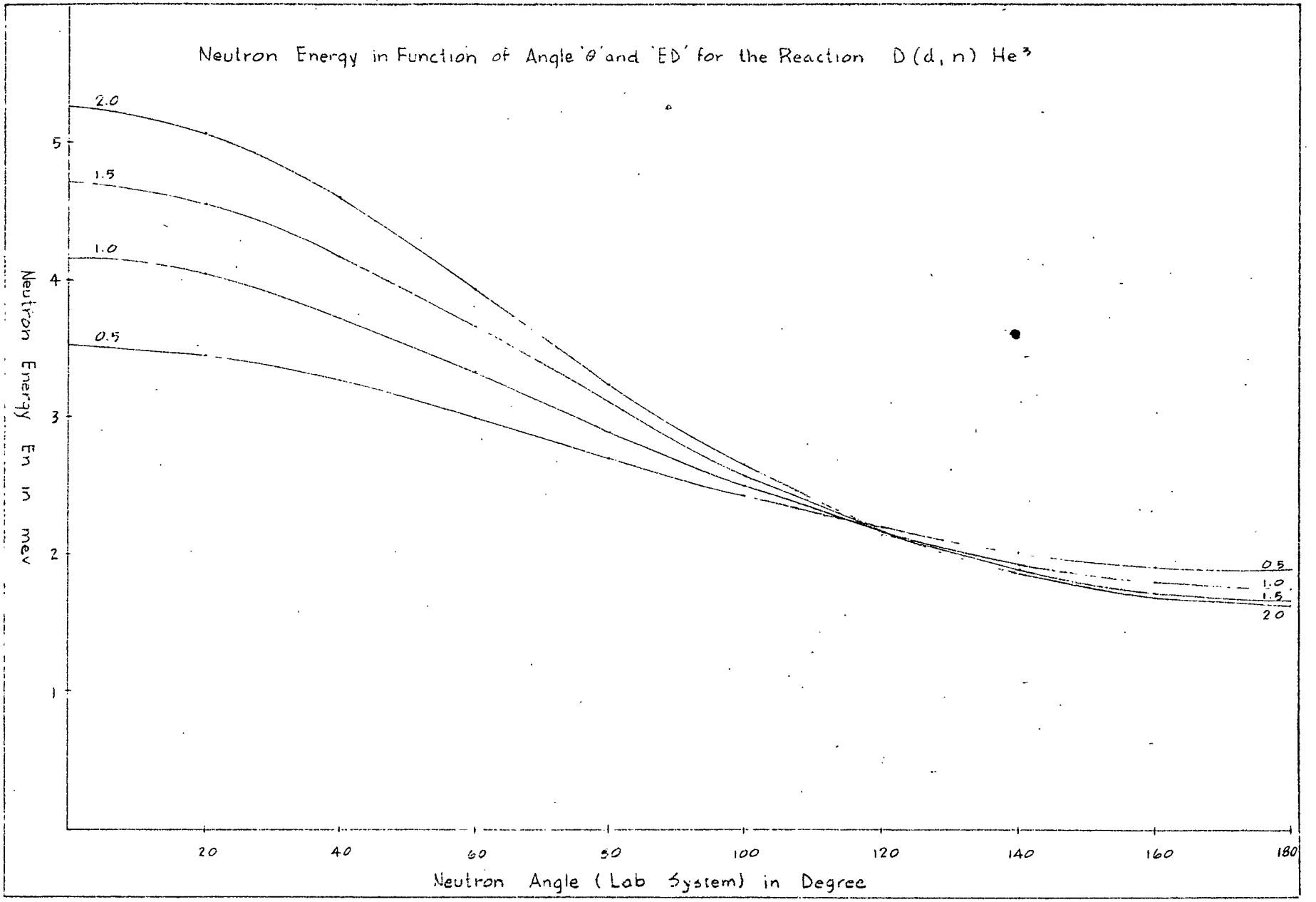
Neutron Energy in Function of Angle 'θ' and 'ED' for the Reaction D (d, n) He³
2.0
1.5
1.0
0.5
Neutron Energy En in mev
1
2
3
4
5
20
40
60
80
100
120
140
160
180
Neutron Angle (Lab System) in Degree

Fig. 4

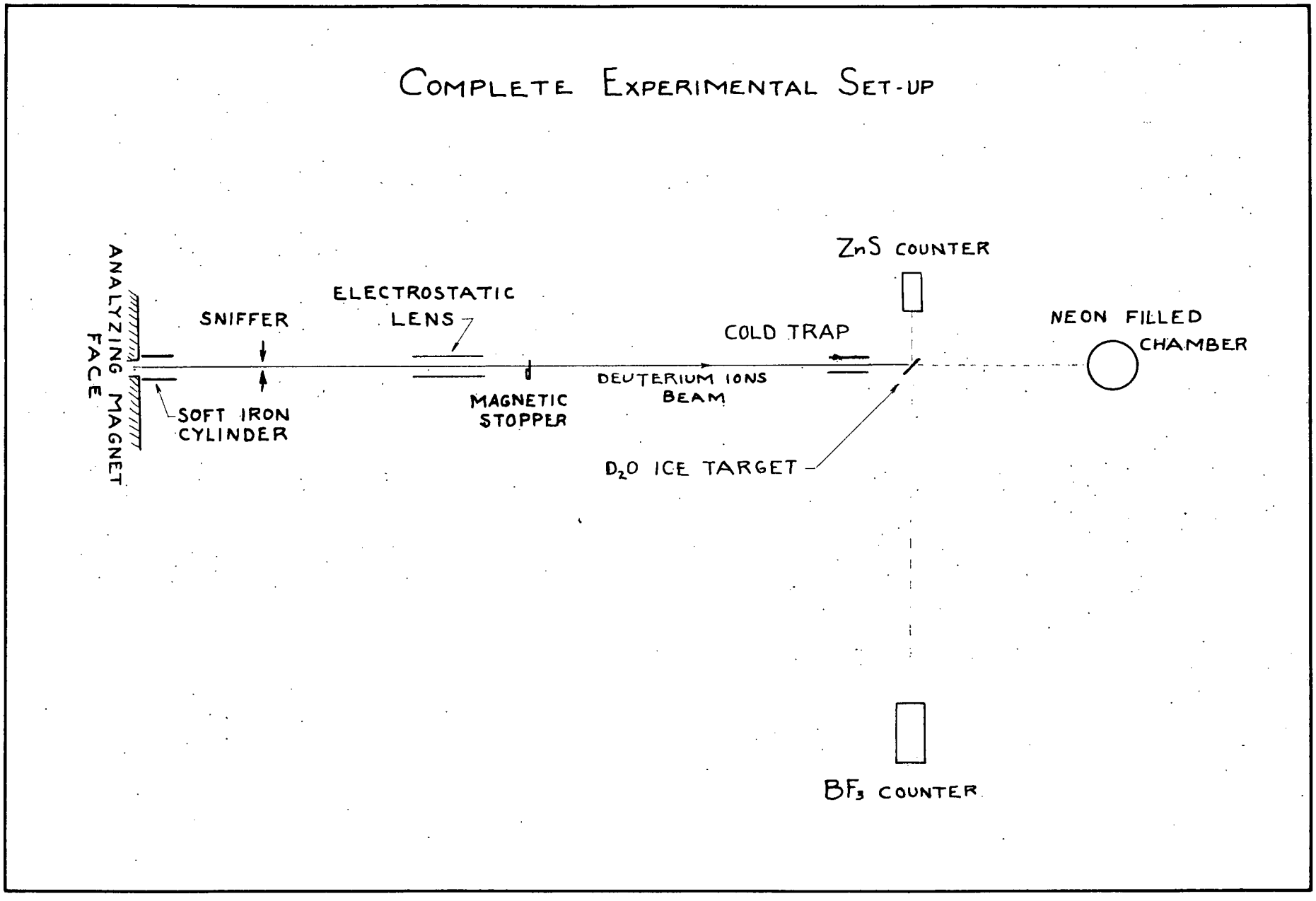
COMPLETE EXPERIMENTAL SET-UP
ANALYZING MAGNET FACE
SNIFFER
ELECTROSTATIC LENS
SOFT IRON CYLINDER
MAGNETIC STOPPER
DEUTERIUM IONS BEAM
COLD TRAP
ZnS COUNTER
NEON FILLED CHAMBER
D2O ICE TARGET
BF3 COUNTER

FIG. 5

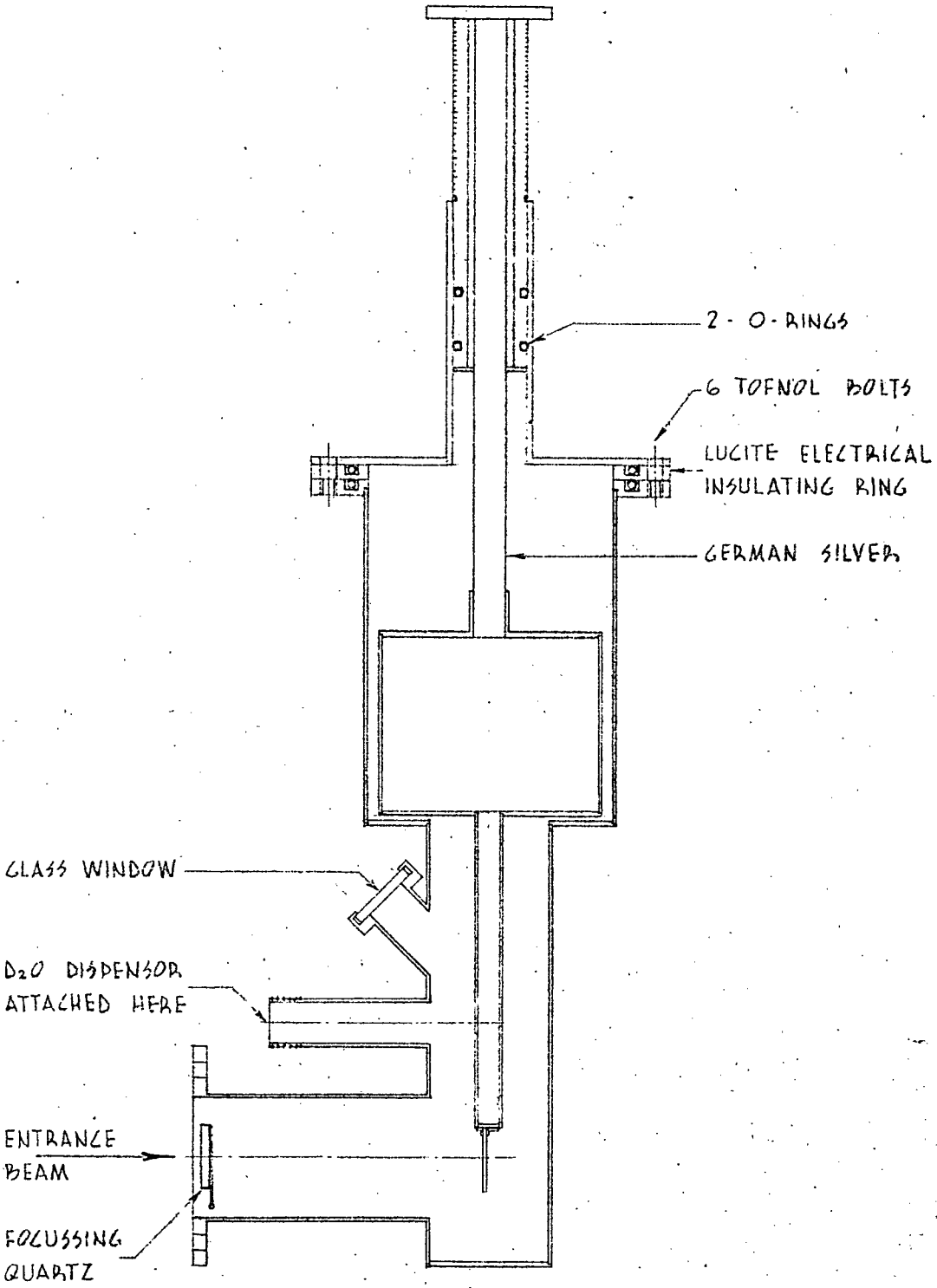

DIAGRAMMATIC SECTIONAL VIEW OF D_2O TARGET POT

Fig. 6

Complete Electronics Set - up

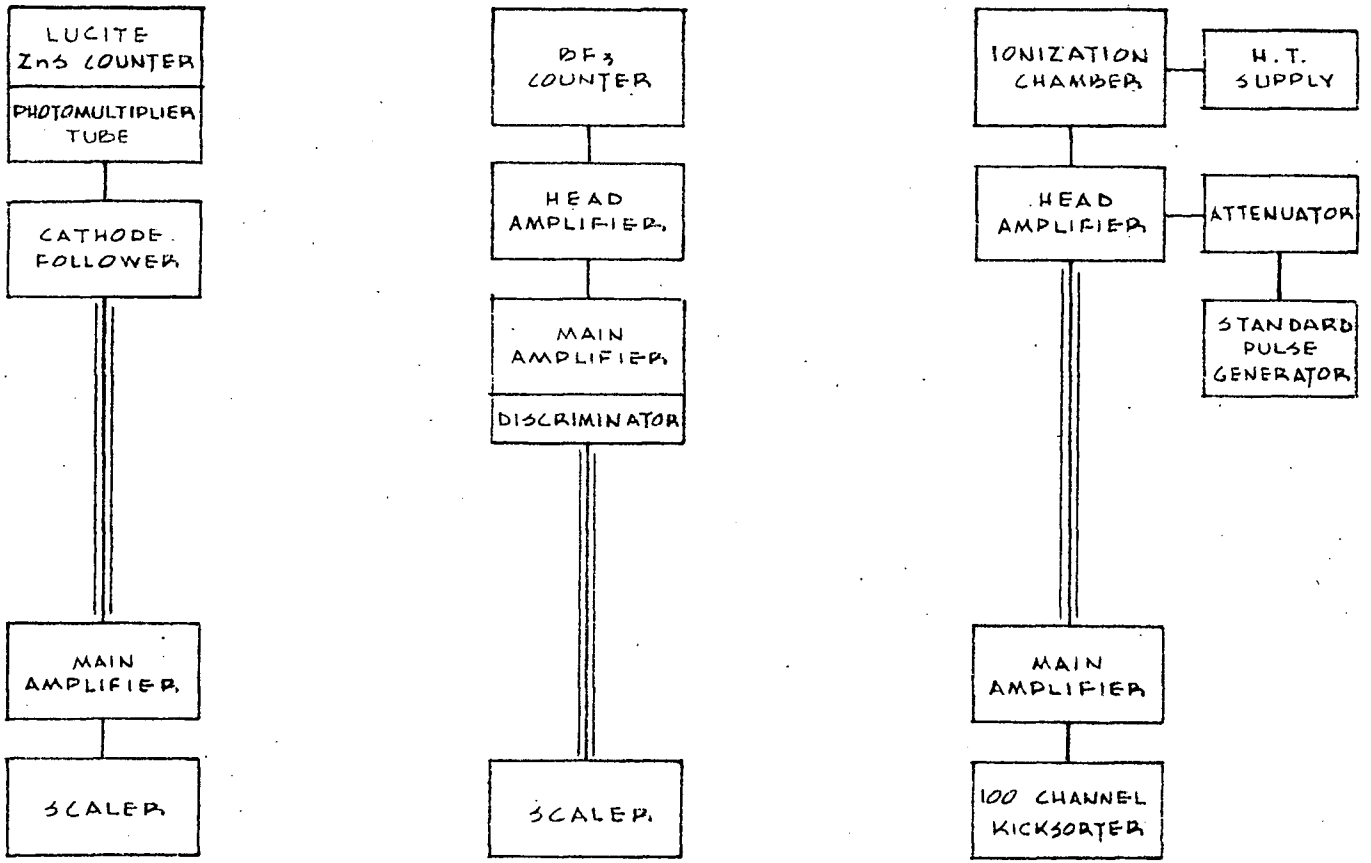

Fig. 7

D_2O Ice Target Thickness Calibration with 6 cm. of octoil, Target at 45°

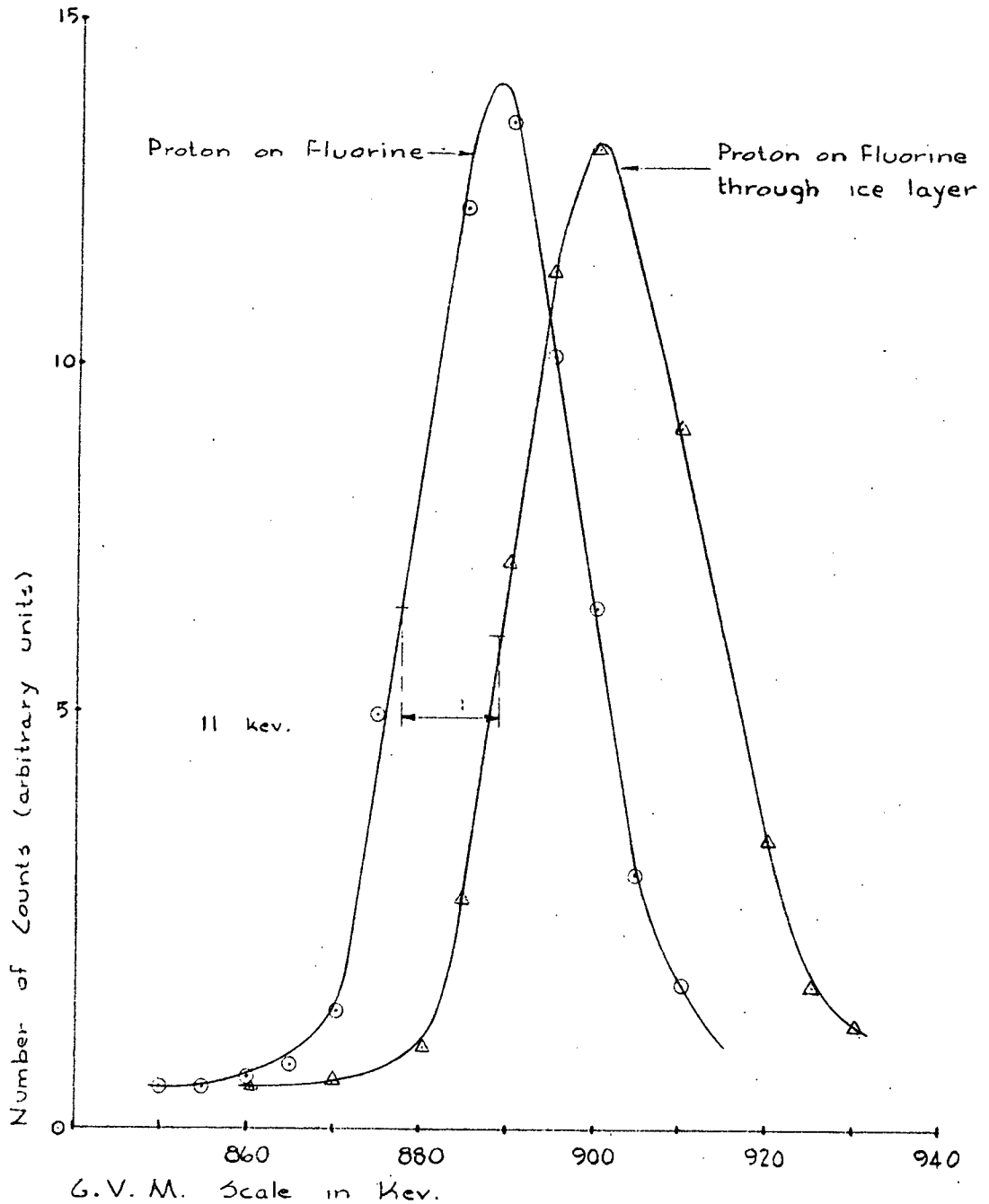

Fig. 8

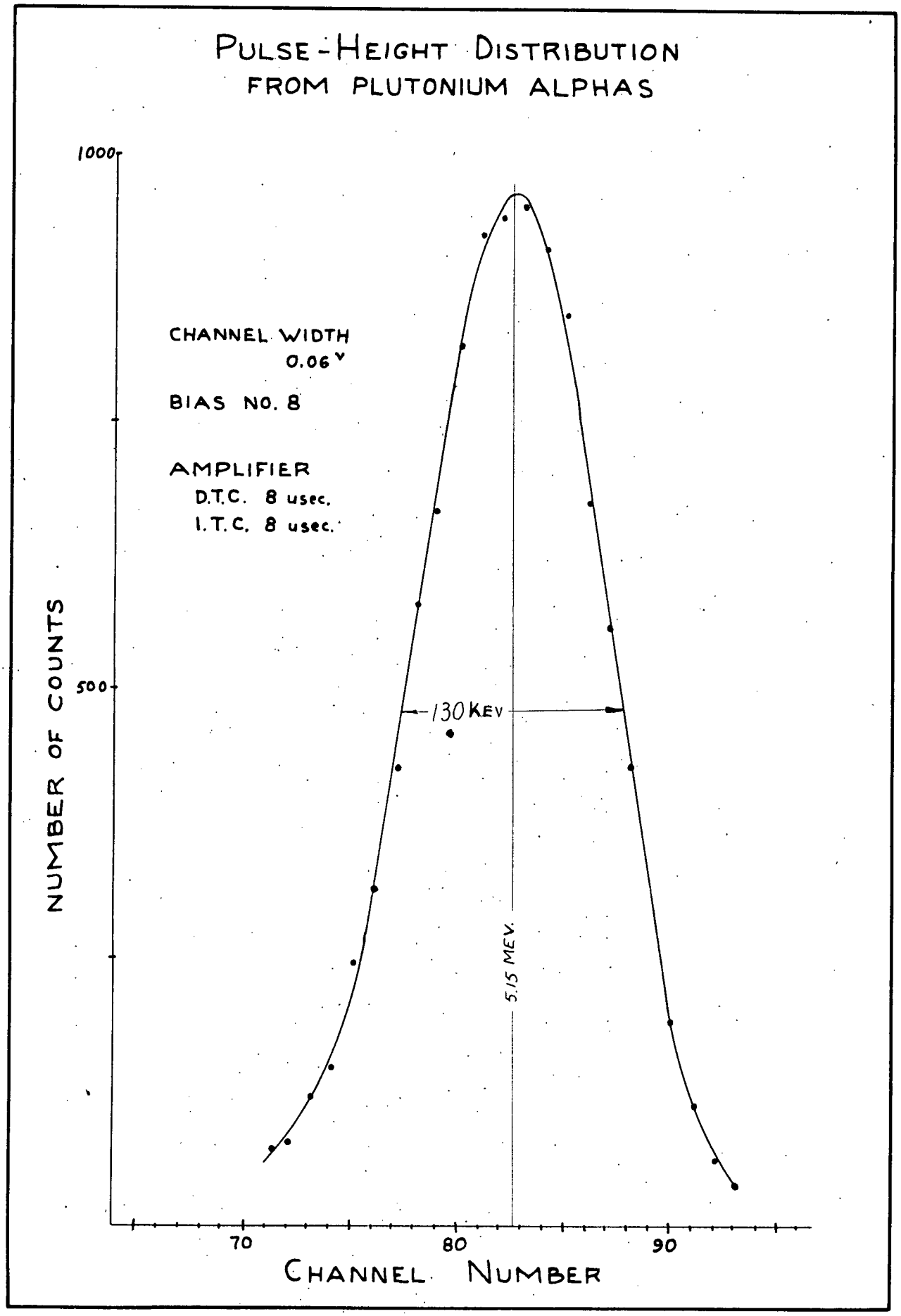
PULSE-HEIGHT DISTRIBUTION
FROM PLUTONIUM ALPHAS
1000
500
NUMBER OF COUNTS
CHANNEL WIDTH
0.06 V
BIAS NO. 8
AMPLIFIER
D.T.C. 8 usec.
I.T.C. 8 usec.
130 KEV
5.15 MEV.
70
80
90
CHANNEL NUMBER

FIG. 9

FIG. 10

ENERGY RESOLUTION OF THE KICKSORTER AT VARIOUS BIAS SETTING BEFORE AND AFTER MODIFICATION

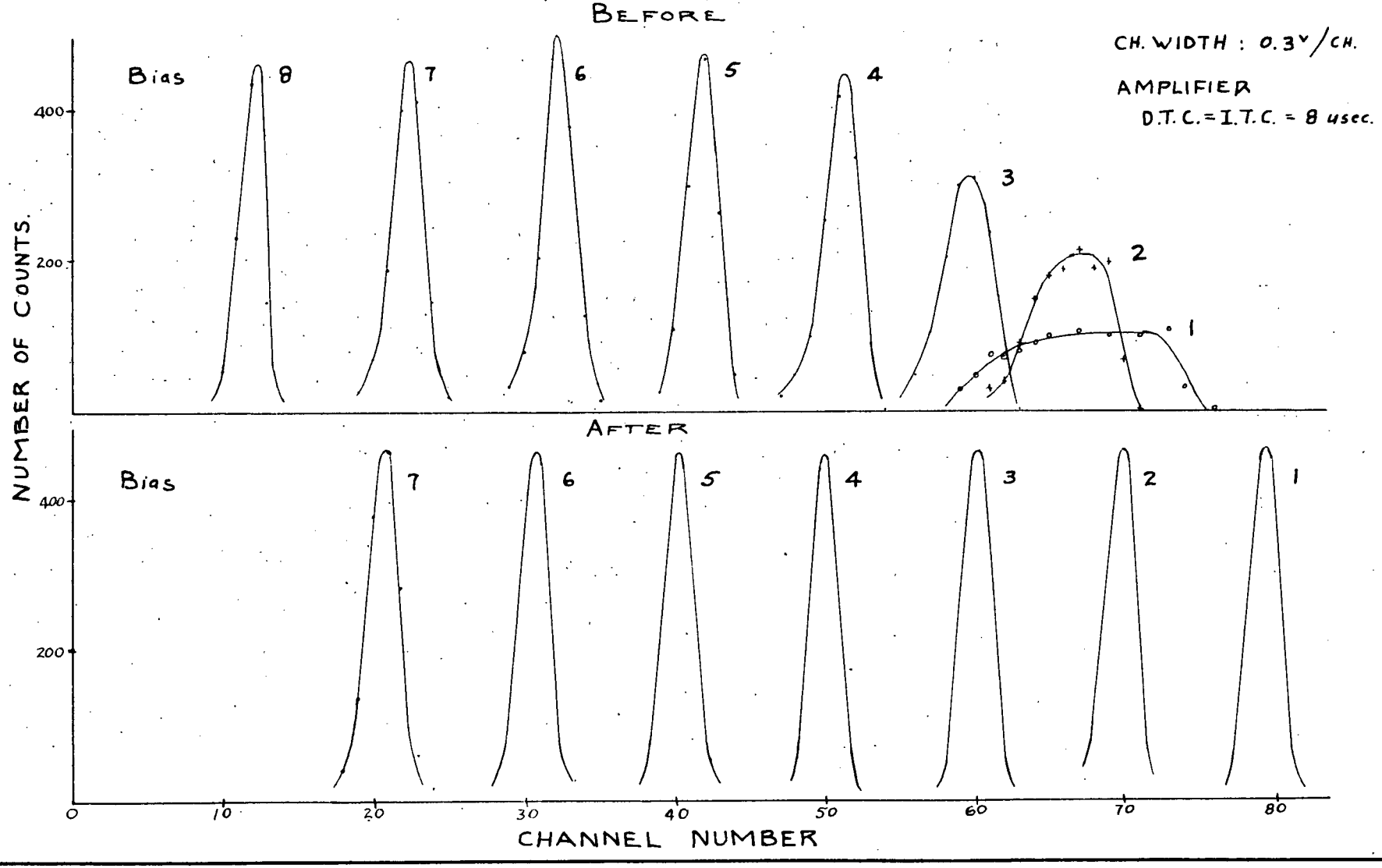

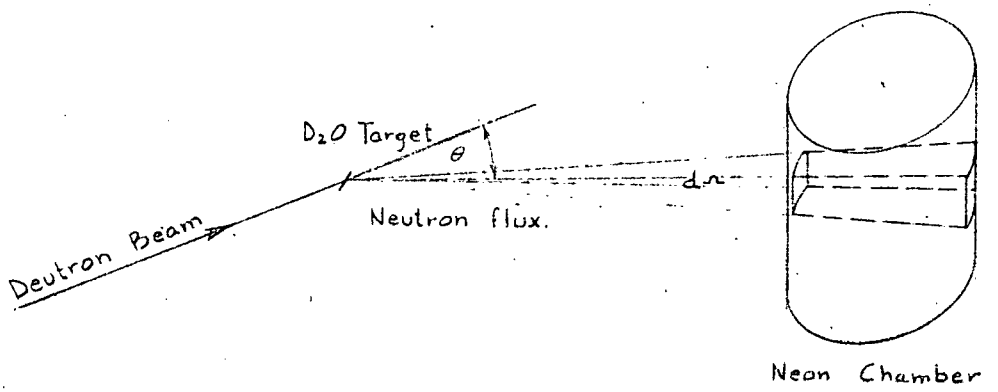
D_2O Target
θ
dx
Deutron Beam
Neutron flux.
Neon Chamber

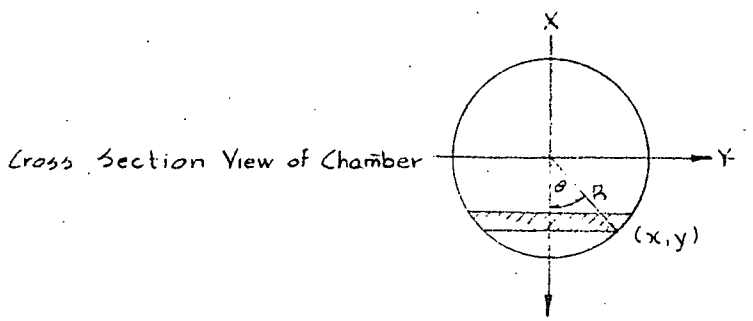
X
Cross Section View of Chamber
Y
θ
R
(x,y)

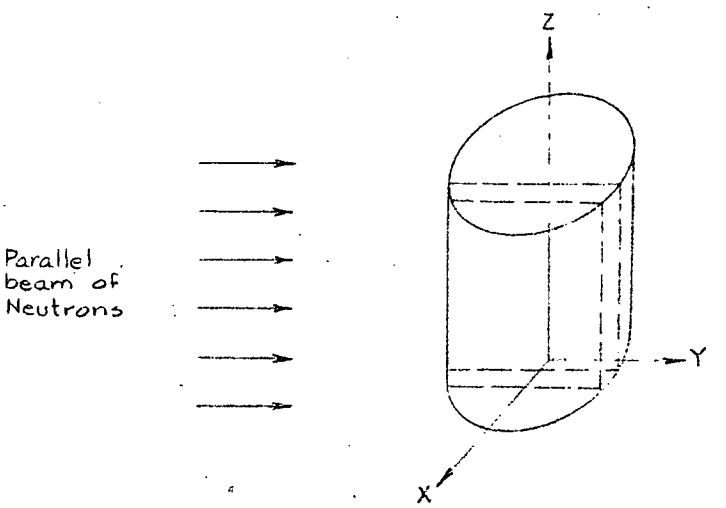
Z
Parallel
beam of
Neutrons
Y
X

Fig. 11

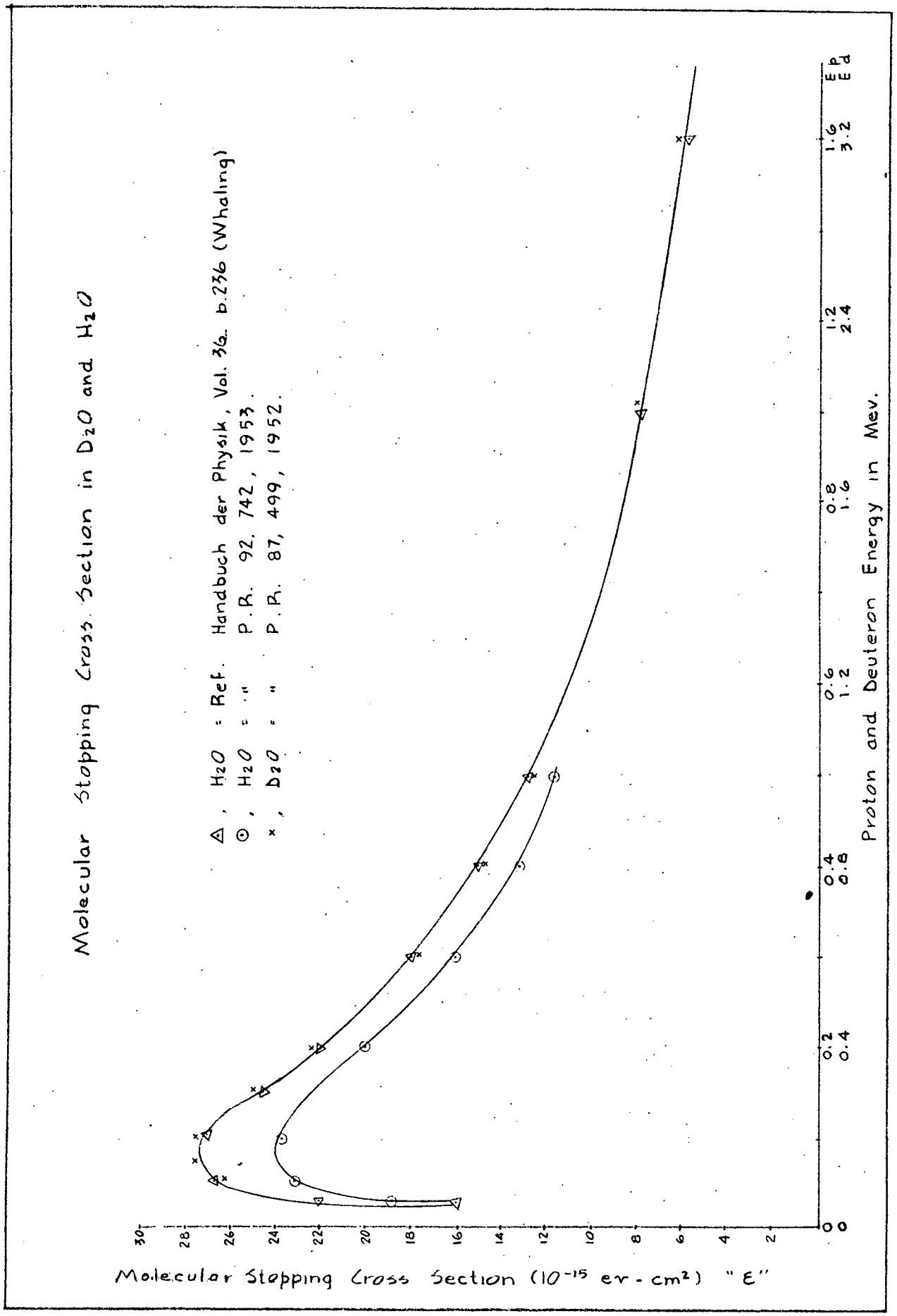
Molecular Stopping Cross Section in D_2O and H_2O
△ , H_2O = Ref. Handbuch der Physik, Vol. 36 b.236 (Whaling)
⊙ , H_2O = " P.R. 92. 742, 1953.
× , D_2O = " P.R. 87, 499, 1952.
Molecular Stopping Cross Section (10^{-15} ev - cm²) "ε"
Proton and Deuteron Energy in Mev.
E_p
E_d

Fig. 12

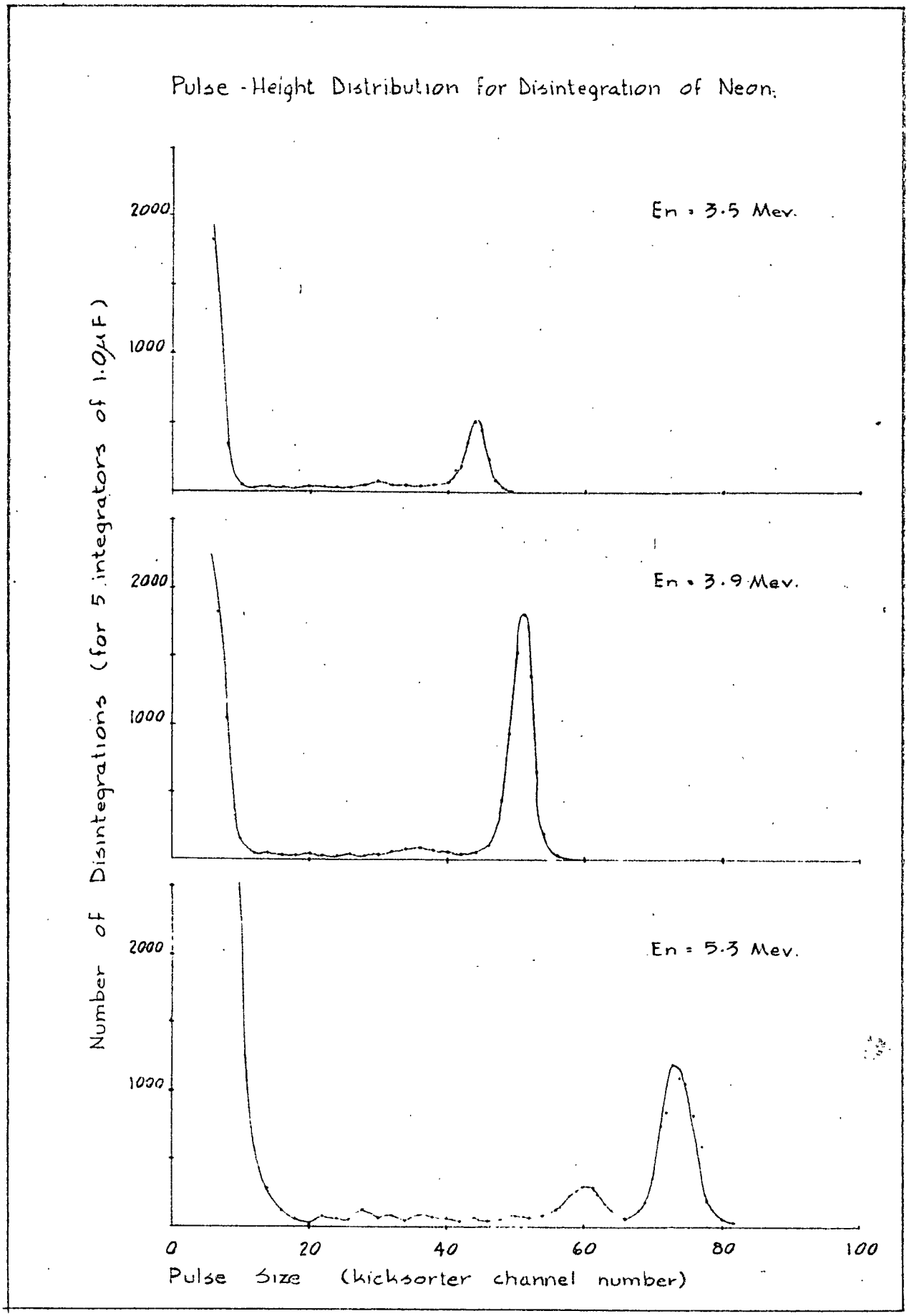
Pulse - Height Distribution for Disintegration of Neon.
En = 3.5 Mev.
En = 3.9 Mev.
En = 5.3 Mev.
2000
1000
Number of Disintegrations (for 5 integrators of 1.0 μF)
0
20
40
60
80
100
Pulse Size (kicksorter channel number)

Fig. 13

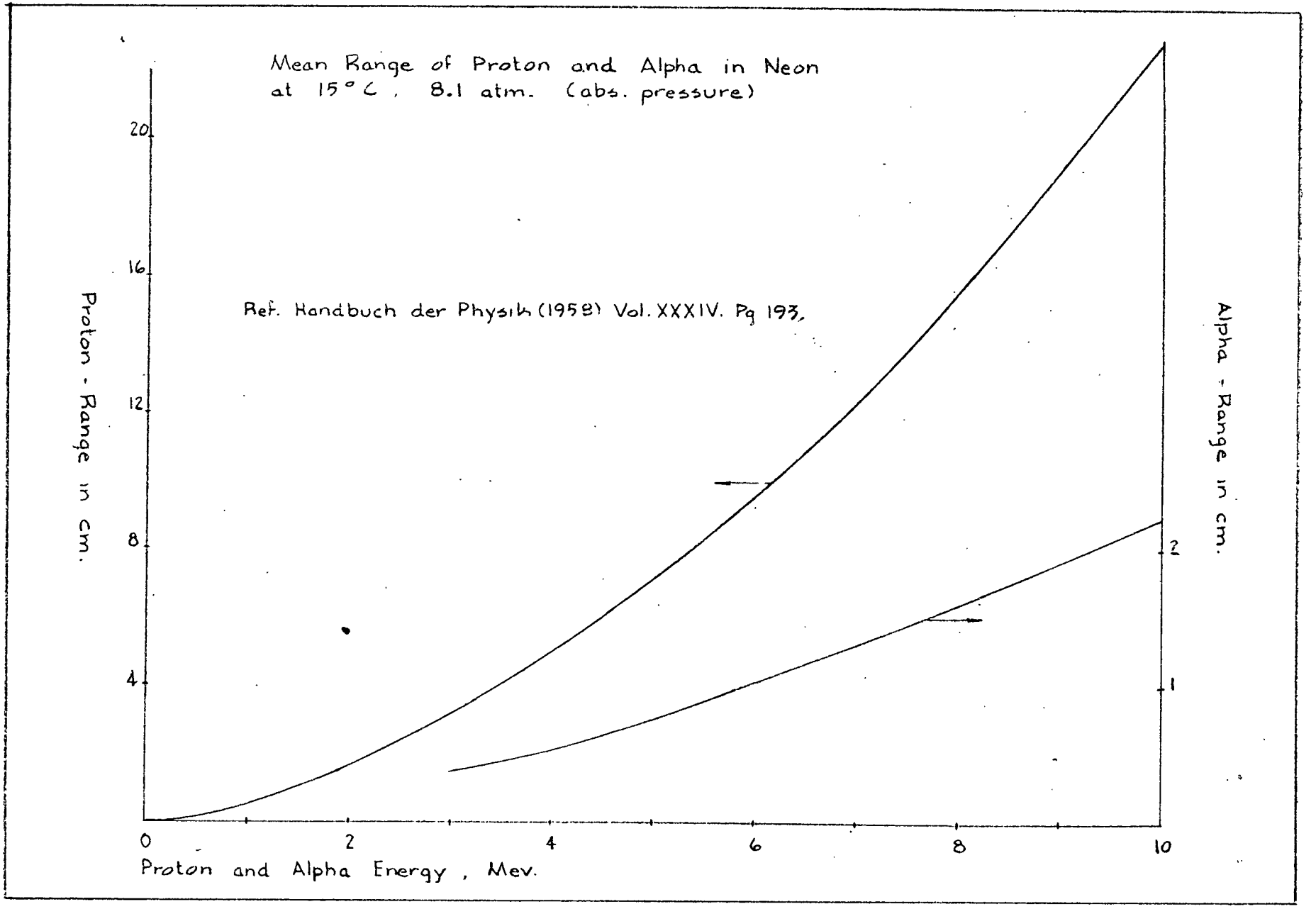
Mean Range of Proton and Alpha in Neon
at 15° C , 8.1 atm. (abs. pressure)
Ref. Handbuch der Physik (1958) Vol. XXXIV. Pg 193,
Proton - Range in cm.
Alpha - Range in cm.
20
16
12
8
4
2
1
0
2
4
6
8
10
Proton and Alpha Energy , Mev.

Fig. 14